Cutting Forces in Turning Operations

Bachelor Thesis

Sergi Martín Umbert

Mechanical Engineer

TFG Treball de Fi de Grau

Norwegian University of
Science and Technology

Department of Mechanical and Industrial Engineering
(MTP)

Summary

At first, the idea of this project was to study internal turning operations in order to earn a better knowledge in the possible deflections suffered by the tools performing these operations. A prediction method of the deflections suffered in finishing operations with variable depths of cut is necessary to achieve high accuracy. In order to study the effects of the deflection in different operations and different tools, a study of the forces received by cutting tools in turning operations has been performed.

In this study, from the basic knowledge of orthogonal cutting until the specific forces received by the tool and the effects that these can generate in the cutting operation have been studied. The geometry of the inserts used in turning operations have been investigated in order to understand the characteristics that affect in the forces received. Moreover, possible problems that can be suffered in these operations such as vibrations or deflection are studied. The main force studied is the radial force, this cutting force has the highest impact in the studied imperfections.

In order to develop a prediction of the cutting forces suffered by the tool, a MATLAB programme has been created with the variable features of tool geometry and cutting conditions. This programme generates a prediction of the chip load area to analyse the forces, it has been tested with different variations to find the most accurate model to predict the cutting forces.

Experimental tests with different inserts and increasing depth of cut have been performed in a lathe with a force measurement system to analyse the empirical differences experienced in the cutting forces. These tests confirm that the radial force presents an increasing behaviour until the depth of cut is greater than the nose radius of the tool, after this moment the force gets stabilized.

Based on the experimental tests carried on, the prediction method elaborated can be compared and used to establish a good relation between the parameters influencing in the radial cutting force and the empirical results. The comparison appears to be suitable and can be used in the prediction of these forces.

A final relation has been studied with the results of the experimental tests. The radial force has been used to predict a deflection in a Silent Tools boring bar. This deflection cause a different depth of cut than the programmed. However, this real depth of cut turns out to present a linear relationship with the programmed.

Acknowledgment

This project has been performed in the framework of an ERASMUS exchange programme in fall 2017. It was performed in the Department of Mechanical and Industrial Engineering (MTP) at the Norwegian University of Science and Technology (NTNU) with supervision of the professor and researcher Knut Sørby. This project was performed as a Bachelor thesis, a one semester long project that has to be written at the end of the Bachelor degree in Mechanical Engineering in the "Universitat Politècnica de Catalunya" (UPC-EEBE).

Expression of thanks

First of all, I would like to express my gratitude to the supervisor of my thesis, the Professor and researcher Knut Sørby, for the helpful guidance and ideas contribute to the accomplishment of this project work.

I would also like to thank the scientist and worker in SINTEF, Vegard Brøtan for the share of knowledge experienced in the tests carried in SANDVIK Teeness As.

And finally, I would like to express my gratitude to the company SANDIVIK Teeness AS for the assistance to the experimental tests performed with Silent Tool Boring Bar, although the calculations could not be used for my project.

Initial Project assignment

Sandvik Teeness developes vibration-damped tools for internal turning operations. Due to the low static stiffness of the tools there is a need for correction methods or in-process measurements to achieve a high accuracy in the turning operations. In this project the student should analyze the problem of finish turning operations in general, and specifically the deflection of slender cutting tools when turning with small depth of cuts. The student should investigate how strain sensors in the tool holder can be used to increase the accuracy and efficiency of turning operations.

List of contents

List of figures

Abbreviations

ϕ_c	Shear angle
ϕ_n	Normal shear angle
θ	Projection angle
β	Average friction angle
α_r	Rake angle
α_n	Normal rake angle
i	Inclination angle
η	Chip flow angle
ψ	Side cutting edge angle
κ	End cutting edge angle
r_e	Nose radius
δ	Deflection
E	Young modulus
A_p	Depth of cut
t_o	Uncut chip thickness
t_c	Deformed chip thickness
w	Width of cut
r_c	Compression ratio
V_c	Cutting velocity
f	Feed rate
A_s	Area of the shear plane
σ_s	Normal stress
τ_s	Shear stress
F_f	Feed force
F_t	tangential force
F_r	Radial force
F_s	Shear force
F_n	Normal force
N	Normal force on the rake
F_u	Friction force on the rake
ϕ_L	Effective lead angle
h	Chip thickness

K	Cutting coefficients
K_m	Modification factor
L_c	Contact edge length

1. Introduction

In a global situation were a complete industrialization is a fact, manufacturing processes have an increasing WEIGHT in order to improve productivity in those industries. However, not only the fact of the velocity in production or the reduction in costs are the only keys of success. Nowadays, a competition for quality results has gained importance over the years, being better or producing better quality finish results in the products released that satisfy requirements and specifications posed by functional demands is a manner to establish a difference, and this difference is only achieved by innovation.

This project performed in collaboration with the Norwegian University of Science and Technology of Trondheim NTNU, namely the Department of Mechanical and Industrial Engineering (MTP) and the company Teeneess AS located in Trondheim, has combined the knowledge of the university research and the real industry work.

The main idea in this project was to continue the studies carried on in finishing turning operations mainly developed in internal turning. These studies were performed in order to achieve better knowledge about the behaviour of slender tools in cutting operations with the goal of obtaining high accuracy results when operating with these tools. High accuracy dimensional properties and good surface quality results are needed in turning specially when complex products are manufactured.

In order to continue these studies a literature research needs to be carried out to understand the factors influencing in this accuracy. Deflections suffered by slender tools have been studied and some tests are carried out in Teeness AS laboratory to analyse them. However, these studies have not been possible to increase due to the lack of facilities in the lab, but the reason of them has been focused.

Therefore, the main study has been focused on the cutting forces that can generate errors in the factors named before. A deep study in the cutting forces in the tool has been carried out and the reasons of this dimensional mistakes has been understood.

2. Theory of metal Machining

Machining is one or more processes in which a piece of raw material is worked by controlled material-removal operations in order to reach the desired design. These operations are often used for elaborating difficult geometries and obtaining final shapes. Most of manufacturing processes are followed by metal-removing operations in order to get the desired final shape, dimension or quality. These processes are also commonly known as Subtractive Manufacturing.

The machining operations can be classified under two major categories: cutting and grinding processes. The most common cutting operations are turning, milling, and drilling followed by special operations such as boring, broaching, hobing, shaping, and form cutting. All metal cutting operations use the same general mechanics, the material is removed by a cutting edge, but with different geometries and application. In the following section, an introduction to the mechanics of cutting is presented. (Altintas, 2012)

2.1. Orthogonal Cutting

In order to achieve the basic knowledge of the mechanics in metal removal, the orthogonal two-dimensional cutting is going to be explained in this section. The material is removed by the cutting tool edge precisely located perpendicular to the workpiece surface. Therefore, in this shaping process the tool's cutting edge is also perpendicular to the direction of the cutting velocity (V_c).

To understand the cutting process, some parameters have to be defined. As an introduction, width of cut (w) and depth of cut (Ap, or Uncut chip thickness represented by t_o in Fig. 1) are two properties that are going to describe the dimension of the metal chip removed.

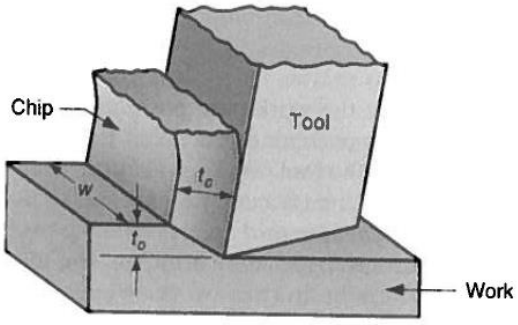

Figure 1: Three dimensional orthogonal cutting representation (Groover, 2011)

In cutting operations it is known that the chip formed flow off as series of parallel plates sliding relative to each other (Groover, 2011). As the chip is formed along the shear plane, the uncut chip thickness increases to the deformed chip thickness (t_c), the relation between them is called the chip compression ratio(r_c). Related as follows (Altintas, 2012),

$$r_c = \frac{t_o}{t_c} \qquad (1)$$

The cutting is assumed to be uniform and the cutting forces are going to be found in the directions of the velocity and the feed rate (*f*). These two forces are called Tangential Force (Ft) and Feed force (F_f). Only orthogonal two-dimensional cut is being explained by now, in oblique cutting a third force appears due to the inclination angle (*i*) of the cutting edge. This force acts in the radial direction, Radial Force (Fr).

In the figures below the deformation geometry caused by the removal operation and the forces generated in it are shown. In this simple explanation, it is assumed that the cutting edge is sharped and without nose radius, so the deformation produced in the shear zone is thin enough.

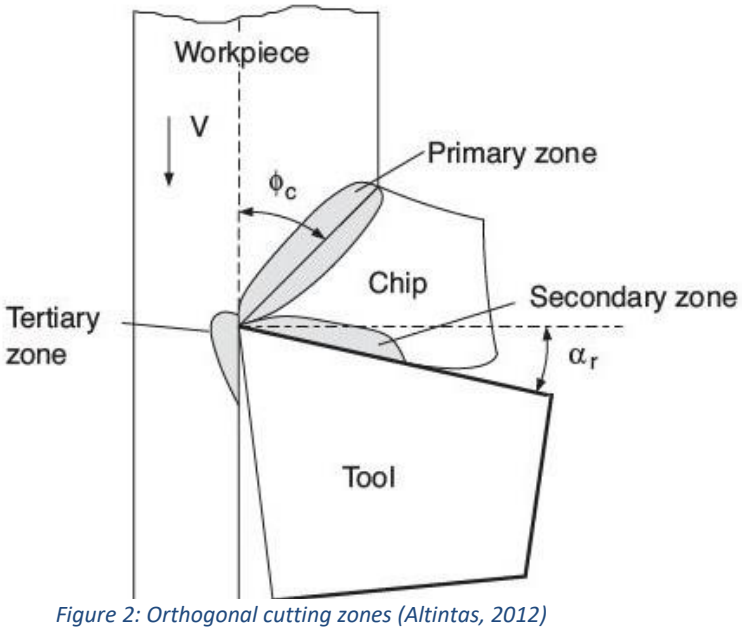

Figure 2: Orthogonal cutting zones (Altintas, 2012)

To describe in a better way the geometry, some parameters are explained. The shear angle ϕ_c is defined as the deviation between the share plane and the direction of the cutting speed. Also,

the rake angle (α_r) of the tool is shown. It is also known that the normal stress (σ_s) and the shear stress (τ_s) are considered constant. (Altintas, 2012)

Force equilibrium is found as the relation between forces. The resultant cutting force is the formed from the tangential cutting force (F_t) and the Feed force (F_f), as presented by (Altintas, 2012),

$$F_c = \sqrt{F_t^2 + F_f^2} \qquad (2)$$

Feed force (F_f) is found in the direction of the uncut chip thickness and Tangential force (F_t) on the direction of the Cutting Velocity (V_c). As the equilibrium theory proves, the tool receives the same forces in equal amplitude but opposite direction (Altintas, 2012).

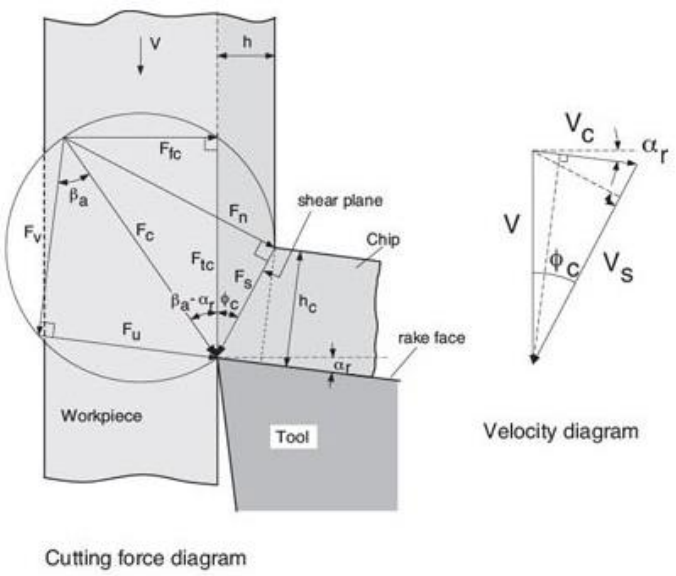

Figure 3: Mechanics of orthogonal cutting (Altintas, 2012)

The velocity diagram (see Fig.3) also called shear strain triangle, is used to derive strain equation.

However, it has to be highlighted that not all forces can be measured directly. In fact, only the forces acting on the tool can be measured directly. Tangential cutting force (F_t) and Feed force (F_f)(also called Thrust force).

The rest of forces are the ones acting in the chip and for calculating them, the relationship between them must be known.

The Shear force (F_s) is the force acting in the shear plane and it can be calculated as (Altintas, 2012):

$$F_s = F_c \cos(\phi_c + \beta - \alpha_r) \quad (3)$$

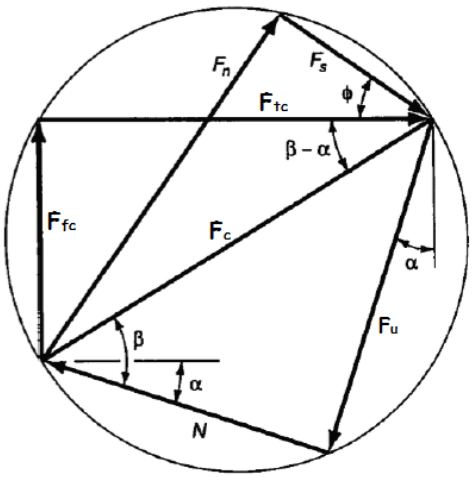

Figure 4: Force diagram in orthogonal cutting (Groover, 2011)

Also, there is a Normal force (F_n) acting on the shear plane and it is similarly described by the equation (Altintas, 2012),

$$F_n = F_c \sin(\phi + \beta - \alpha) \quad (4)$$

Two components of the cutting force belonging to the secondary shear zone are acting directly on the rake face of the tool. The normal force (N) and the Friction force (F_u) on the rake face are presented as follows (Altintas, 2012):

$$N = F_t \cos \alpha_r - F_f \sin \alpha_r \quad (5)$$

$$F_u = F_t \sin \alpha_r - F_f \cos \alpha_r \quad (6)$$

Shear stress (τ_s) is the component of stress that is coplanar with the shear plane surface. As it is assumed, the shear stress is determined as follows (Altintas, 2012):

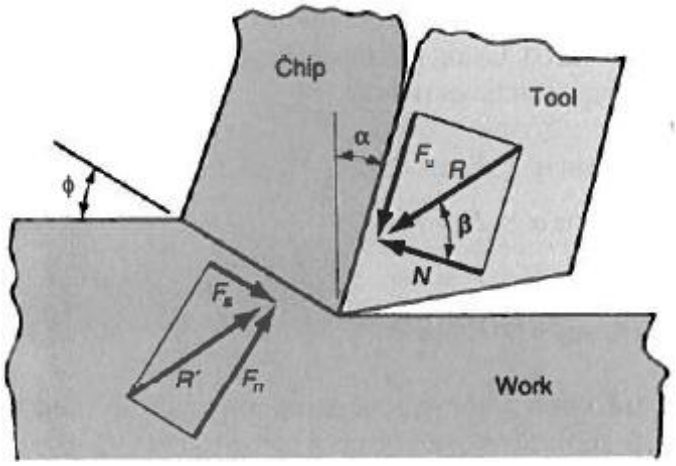

Figure 5: Forces acting in the chip (Groover, 2011)

$$\tau_s = \frac{F_s}{A_s} \qquad (7)$$

Where A_s is the Area of the shear plane and it is determined by (Altintas, 2012):

$$A_s = w\frac{h}{\sin\phi} \qquad (8)$$

Where *w* is the width of cut and *h* the uncut chip thickness (depth of cut in turning).

In the moment when the shear angle is needed the (r_c) ratio must be calculated. The shear angle is found from the geometry as a function of the rake angle and the chip compression ratio as (Altintas, 2012),

$$\phi = \tan^{-1}\frac{r_c\cos\alpha}{1-\sin\alpha} \qquad (9)$$

As it is known, orthogonal cutting cannot be directly applied to practical cutting calculations due to numerous facts such as tool geometry, workpiece material or chip breaking grooves. It is recommended to carry on some experiments to determine the constant parameters of the cutting operations.

Moreover, oblique cutting mechanics and plasticity analysis are needed to establish the real behaviour of a particular cutting process.

2.1.1. Prediction of shear Angle

In order to achieve a theoretical calculation of the Shear Angle, the minimum energy principle proposed by (Merchant, 1945) it is used. Basically, the workpiece is going to select a shear angle (ϕ) that minimizes energy which determines a larger shear angle than the highest shear stress principle.

$$\phi_c = 45 + \frac{\alpha_r}{2} - \frac{\beta}{2} \qquad (10)$$

This equation presents an important relationship between the shear angle (ϕ_c), the rake angle (α_r) and the friction coefficients between the workpiece and the cutting tool (tan β). The increment of the shear angle generates an increase of the cutting forces and the power consumed. (Merchant, 1945)

2.2.Mechanics in oblique cutting

In this section the mechanics of oblique cutting are being introduced. Oblique cutting is a different type of cutting in which the tool's cutting edge make an angle (*i*) with the direction of tool motion. This will affect the cutting conditions and redirect the cutting forces. It is also known as 3D cutting because the cutting forces developed during cutting cannot be represented by 2D coordinate.

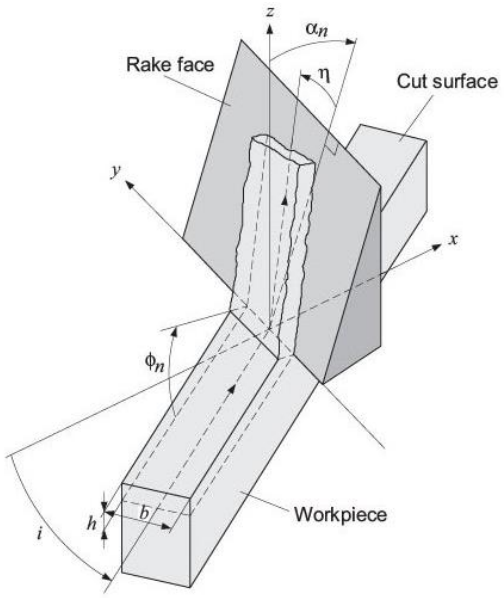

Figure 6: Geometry of Oblique cutting (Altintas, 2012)

In oblique operations, the cutting velocity (V_c) has an oblique or inclination angle (*i*). Therefore, the directions of shear, friction, chip flow, and resultant cutting force vectors have components in the three Cartesian coordinates (x,y,z). The important planes in oblique cutting are the shear plane, the rake face, the cut surface *xy*, the normal plane and the velocity plane.

It can be considered that the mechanics of oblique cutting in the normal plane are equivalent to the orthogonal cutting with a projection depending in the inclination angle (*i*).

Some of the important angles and forces need to be explained in order to understand the mechanics of this operations.

The normal shear angle (ϕ_n) is the angle between the shear and xy planes. In the other hand, the oblique shear angle (ϕ_i) is the angle made between the shear velocity and the vector normal to the cutting plane on the normal plane.

The sheared chips flow over the rake face with an angle called chip flow angle (η), normal to the cutting edge and its known to lie on the normal plane (P_n). The normal rake angle (α_n) is the angle between the Z axis and the normal vector on the rake face.

After the introduction of the geometrical angles needed, forces must be introduced.

There is an existent friction force created in the operation and it has the same direction as the chip flow. The resultant cutting force created in these operations is generated from the friction force on the rake face (F_u) and the normal force on the rake (N) with a friction angle between them (β). The resultant force vector has a projection angle (θ) with the normal plane (P_n), which at the same time has an angle of $\beta+\alpha$ with the normal force. (Altintas, 2012)

There have been numerous proposed solutions based on empirical results in chip flow direction and other empirical assumptions. In this paragraph, the focus is on the prediction of the shear direction based on the law of mechanics. Therefore, a summary of the most important principles is introduced.

Maximum shear principle:

To predict the direction of the shear angle in orthogonal cutting, the maximum shear criterion is applied. It is assumed that the shear happens when the angle between the shear velocity and the resultant force is 45˚ (the maximum shear stress direction). In oblique cutting, this same principle can be applied. (Altintas, 2012)

Furthermore, the principle requires that the projection of the resultant cutting force to the shear plane, coincides with the shear direction. Otherwise, the shear stress is not the maximum on the shear plane. It must be mentioned that the angles of friction (β), rake (α_n), and inclination (*i*) depend on the geometry and material tests.

Minimum Energy principle:

A different prediction for the shear angle is proposed by (Merchant, 1945), the theory consist in applying the minimum energy principle to orthogonal cutting and then extend it to oblique cutting.

It is known, that the shear force is expressed as a projection of the resultant cutting force in the direction of the shear or as a product of shear stress and shear plane area. This minimum energy principle requires the cutting power to be minimum for a single shear angle solution.

A numerical iteration is carried on until the non-dimensional cutting power converges to the minimum.

Empirical Approach (Armarego, 1993)

There is a large number of empirical approaches, but in this paragraph the one proposed by (E.J.A.Armarego & R.C.Whitfield, 1985) is introduced. In this principle, two assumptions are made on the shear direction and chip length ratio. First, the shear velocity must be collinear with the shear force and second, it is assumed that the chip length ratio is the same as in orthogonal cutting. It has also to be noticed that by combining geometric equations we get ($\beta = \theta + \alpha_n$).

2.3.Prediction of cutting forces

The cutting force components are found to be projections of the resultant cutting Force (F_c). These forces are declared as a function of shear yield stress (τ), resultant force direction (θ_n, θ_i), oblique angle (i), and oblique shear angles (ϕ_n, ϕ_i).

The force components are in the directions of cutting speed (F_t), Thrust (F_f) and normal direction (F_r). With these forces and (E.J.A.Armarego & R.C.Whitfield, 1985) classical oblique model, the corresponding cutting constants can be found using geometric relations (Altintas, 2012).

$$K_{tc} = \frac{\tau}{\sin\phi_n}\frac{\cos(\beta_n-\alpha_n)+\tan i\tan\eta\sin\beta_n}{\sqrt{\cos^2(\phi_n+\beta_n-\alpha_n)+\tan^2\eta+\sin^2\beta_n}}$$
$$K_{fc} = \frac{\tau}{\sin\phi_n\cos i}\frac{\sin(\beta_n-\alpha_n)}{\sqrt{\cos^2(\phi_n+\beta_n-\alpha_n)+\tan^2\eta+\sin^2\beta_n}} \quad (11)$$
$$K_{rc} = \frac{\tau}{\sin\phi_n}\frac{\cos(\beta_n-\alpha_n)\tan i-\tan\eta\sin\beta_n}{\sqrt{\cos^2(\phi_n+\beta_n-\alpha_n)+\tan^2\eta+\sin^2\beta_n}}$$

This practical approach can be used in predicting the oblique cutting forces from the orthogonal cutting. In this procedure, an evaluation of the shear angle(ϕ_c), average friction angle(β) and shear yield stress has to be done from the orthogonal cutting.

It is assumed that the orthogonal shear angle is the same as the normal share angle in oblique cutting ($\phi_c = \phi_n$), same relation used for the rake angle ($\alpha_r = \alpha_n$) and the chip flow angle is equal to the oblique angle ($\eta = i$). In this procedure, it is also considered that the friction coefficient(β) and the shear stress in both orthogonal and oblique cutting operations in the same work parameters.

2.4.Turning Process

A turning operation is a machining process used to machine cylindrical parts. The tool normally moves along the main axe (z) while the workpiece rotates. When configurated with a lower diameter than the actual of the workpiece, it reduces the diameter of it by cutting the "surface" of the workpiece. It can also move perpendicular to the main axe, this operation is normally used only for removing material from the flat face (facing) or for removing a specific part from the total length (Cut-off).

The cutting operation is produced with the displacement of the tool, the removal of a thin section of the surface reduces the diameter of the workpiece. A diagram of the standard turning process forces is shown in the figure below, where it can also be seen the parallel direction of the cutting tool and the spindle velocity.

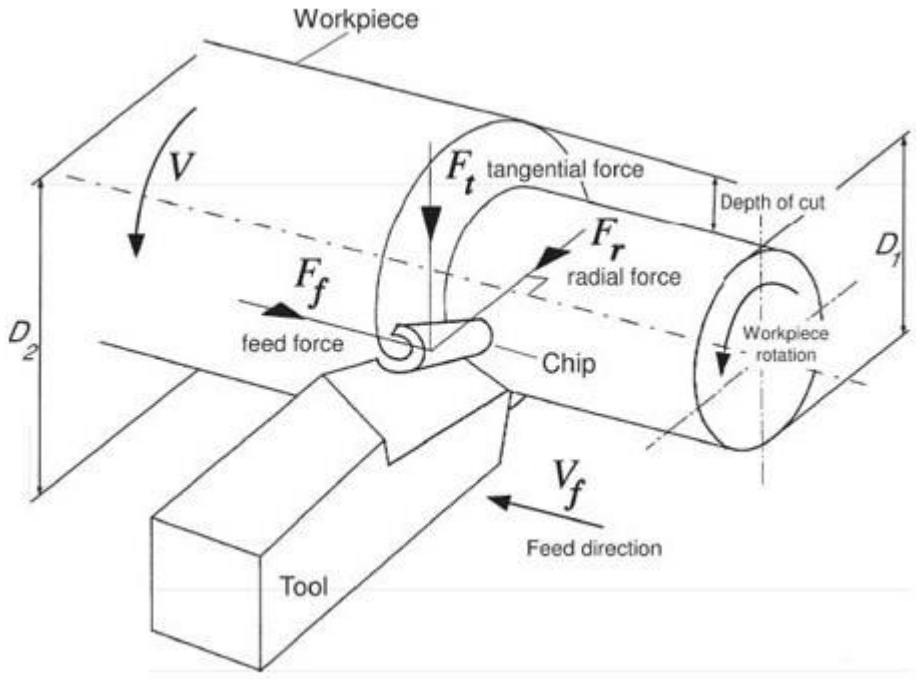

Figure 7: Geometry of a turning process (Altintas, 2012)

Some considerations have to be attended when a good accuracy and surface finish needs to be achieved. Clamping stability and correct centre height are two of these important factors in order to maintain a good operation quality. The centre height affects both the rake angle and cutting force on the tool. When machining with long overhangs, correct clamping must be exceptional, however, possible dimensional mistakes have to be considered due to tool or workpiece deflection.

In the following section, the standard tool geometry and important geometric parameters influencing in the turning process are being explained. These parameters are the nose radius, side rake angle, back rake angle and side cutting edge angle. As an important introduction, it is assumed that the chip produced in the turning operation comes off and slides on the rake face of the tool. Positive rake angles make higher shear angles, so the cutting forces are reduced, and the chip can flow easily, hence it leaves a better surface finish.

2.5.Tool geometry

In machining, tool geometry is an important aspect to consider due to its influence in cutting forces dimensions and chip formation behaviour. Moreover, these factors will directly affect to other issues such as tool deflection, vibration, etc.

The most important geometrical parameters are included in the figure below. These parameters are the side cutting edge angle, end cutting edge angle, cutting edge inclination and the nose radius.

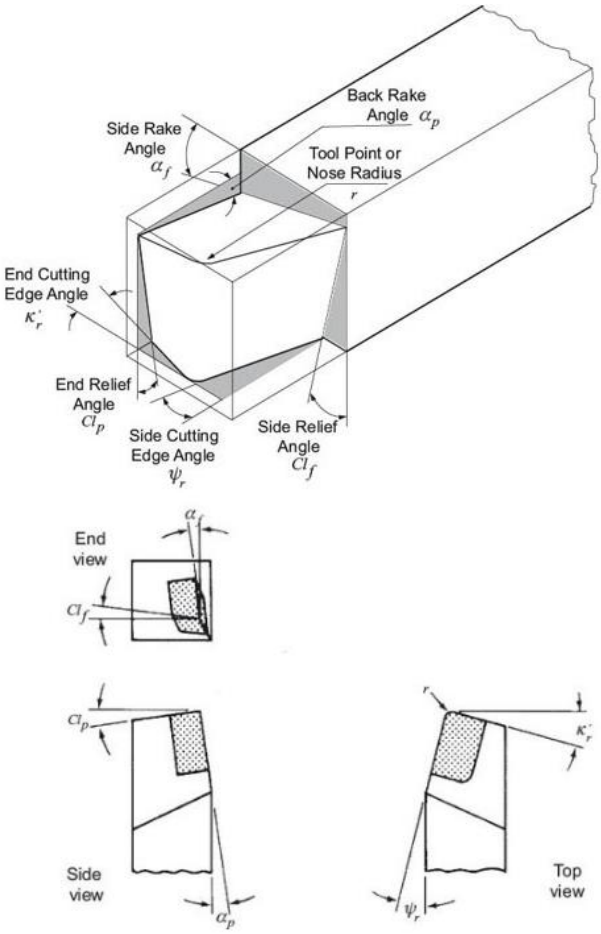

Figure 8: Geometry of a turning tool (Altintas, 2012)

2.5.1. Side cutting edge angle

Side cutting edge angle (ψ) is the angle between the side cutting edge and the axis of the tool. It is used to reduce impact load and is also useful for a better distribution of the forces along the cutting tool. Chip thickness, feed and radial forces can be controlled by the correction of this parameter.

Increasing the side cutting angle produce an enlargement of the chip contact length and decreases chip thickness. Therefore, cutting forces are dispersed acting in a longer cutting surface and in different directions. Depending on the direction of this angle, it can make reduce or increase the radial forces (Mitsubishi Materials Corporation, s.f.).

Therefore, thin and slender tools/workpieces can suffer from bending problems. Modification of the side cutting angle is a useful measure to avoid undesired radial forces and prolong tool's life. Thus, rigidity of the machine is also important when considering changing this angle. Side cutting angle producing big forces in radial direction is not recommended in low rigidity machines.

2.5.2. End cutting edge angle

End cutting edge angle (Ķ) is the angle, the end cutting edge makes with the width of the tool. It is normally used to avoid interference between the machined surface, often with difficult and irregular shapes, and the tool. Usually the end cutting angle goes from 5° to 15°.

Decreasing the end cutting edge angle increases cutting edge strength but also increases forces in the back part of the tool, that can cause chattering and vibrations during the cutting operation. Edge temperature is also increased by decreasing this angle.

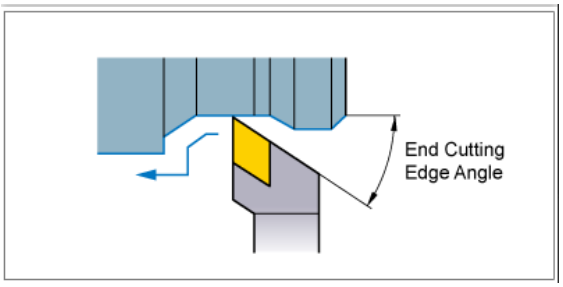

Figure 9: End cutting edge angle ilustration (Mitsubishi Materials Corporation, s.f.) (Mecholic, s.f.)

2.5.3. Cutting edge inclination (Rake angle)

The rake angle indicates the inclination of the rake face, inclination towards the edge of the tool, which is perpendicular to the surface of the workpiece in turning.

The cutting edge receives a heavy impact at the beginning of each cut, this inclination protects the tool's cutting edge from receiving the whole impact and avoids fracturing.

Cutting edge inclination is also important for chip formation and the disengagement of it.

A large rake angle reduces the tool's cross section, area of the tool that absorbs the heat. This can make the tool become weak and reduce its life.

This angle is composed by two different angles:

- Back rake angle: is the slope given to the face or the surface of the tool. This slope is given from the nose along the length of the tool.
- Side rake angle: This slope is given from the nose along the width of the tool.

A negative cutting edge inclination makes the chip flow in the workpiece direction. Otherwise, a positive cutting edge inclination disposes the chips in the opposite direction, flowing out of the operation.

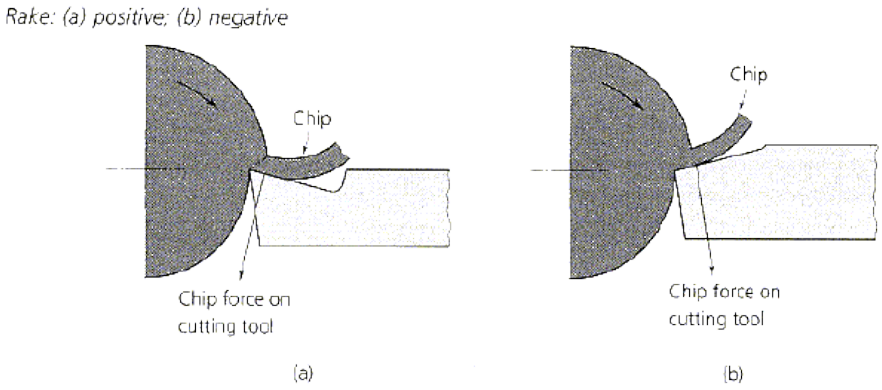

Figure 10: Positive and negative rake angle (Mecholic, s.f.)

Positive rake angle geometry is suitable for machining soft, ductile materials (Ex: aluminum) and negative is for cutting hard materials, where the cutting forces are high (Hard material, high speed and feed). It can also affect in matters of chattering and vibrations as a result of the increment of back forces due to a negative cutting inclination. By the way, this property can also increase the cutting edge strength.

2.5.4. Nose radius

Nose radius is probably the most important characteristic about the tool geometry. It is the angle between the side cutting edge and the end cutting edge. The selection of it depends on the depth of cut (Ap) and the feed rate (f), and influences in the surface finish, the insert strength and the chip breaking.

Nose radius also affects in the chip formation, at the same feed rate, a smaller nose radius generates a better chip breaking. A small nose radius is recommended for small depths of cut. The insert strength is reduced but also undesired radial forces that can produce vibrations are avoided. However, while a large corner radius and small federate create good surface, small corner radius and large feed rates leave more material behind causing a rougher finish.

In the other hand, a big nose radius can be useful if higher values of feed rate or depth of cut are required. This factor will increase the insert strength but also can lead to increased radial forces.

It is assumed that axial forces are preferred to radial forces. Radial forces can lead to bending, chattering or vibrations and therefore, poor surface finish. As higher the depth of cut, higher axial forces and lower radial (see Fig.11).

Figure 11: Force relation with depth of cut (CADEM NCyclopedia multimedia, s.f.)

2.6.Factors influencing in vibration

Vibration is one of the most common problems concerning metal machining and specially when trying to accomplish good surface finish or a high accuracy dimension. Various factors are known to be influencing in the generation of these undesired vibrations, some of them are going to be explained in this paragraph.

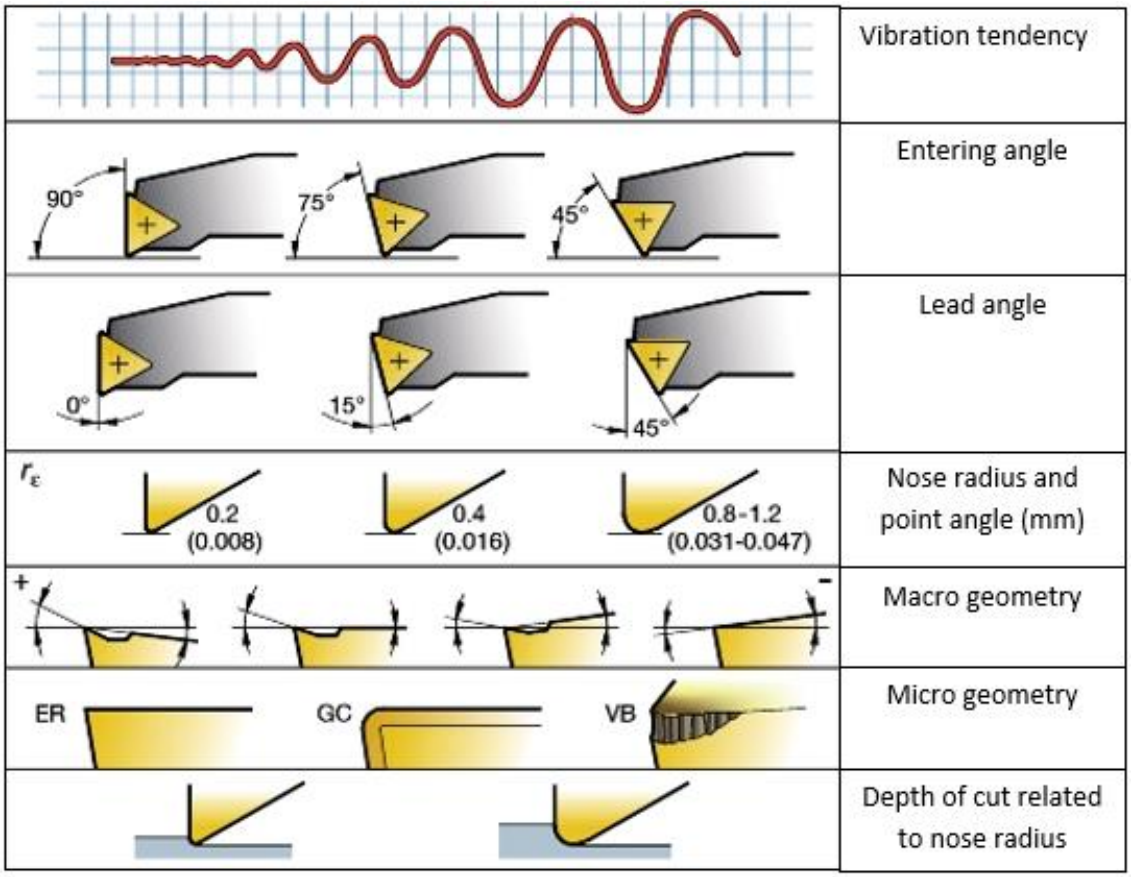

Figure 12: Factors influencing in vibration (SANDVIK Coromant, s.f.)

As it is assumed, radial forces are the main problem in matters of radial deflection and vibration. Therefore, factors influencing in these forces must be strictly controlled. Potential measures to minimize vibration tendencies:

- Large entering angle and positive rake face
- Small nose radius and point angle
- Positive macro geometry
- Controlled wear pattern and ER-treatment on the micro geometry.
- Larger depth of cut than the nose radius, making sure the proper distribution of forces.

The re-direction of forces is a crucial issue when reducing deflection. A side cutting angle as close as 90 as possible, maximize the portion of feed force coming back from the workpiece in the axial direction. Therefore, the deflection will be remarkably lower.

Machining with a side cutting angle higher than 90˚ is highly recommended when machining with a boring bar and a higher depth of cut than the nose radius. Thus, the axial forces will predominate among the radial. For internal turning, this angle can never be less than 75˚ (SANDVIK Coromant, s.f.).

If the operation is being carried below the nose radius, the side cutting angle is no longer relevant, different side cutting angles will give equal results.

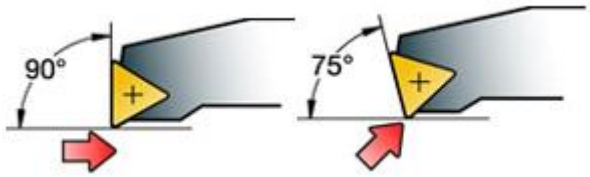

Figure 13: Side cutting edge angle (SANDVIK Coromant, s.f.)

Also, as it has already been explained, as more positive the rake angle, more reduced the cutting forces needed for machining the component. Therefore, the most positive geometry must be chosen, with a suitable chip-breaker for cutting data. However, this may also decrease the wear resistance and edge strength, as well as the chip-control.

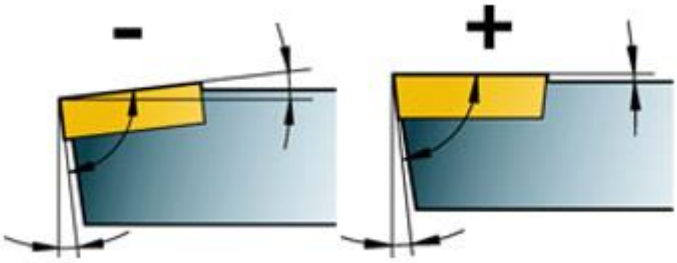

Figure 14: Negative and positive rake angle (SANDVIK Coromant, s.f.)

2.7.Workpiece material

In machining, the material of the workpiece used should be taken into account in order to predict the forces and reactions that the cutting operation will suffer. When talking about cutting forces, power or torque, the specific cutting force (k_{c1}) is used. It is explained as the force that generates in the cutting direction (see picture) needed to cut a chip with an area of 1mm^2 and a thickness of 1 mm. This value will not be the same for the different groups of steel and also can vary depending on the composition of it.

This value is representing a cut with a neutral insert with a rake angle α= 0˚, with a other values this angle will be different. This value will vary, for example, if the rake angle is more positive than 0 degrees, the actual kc value will decrease.

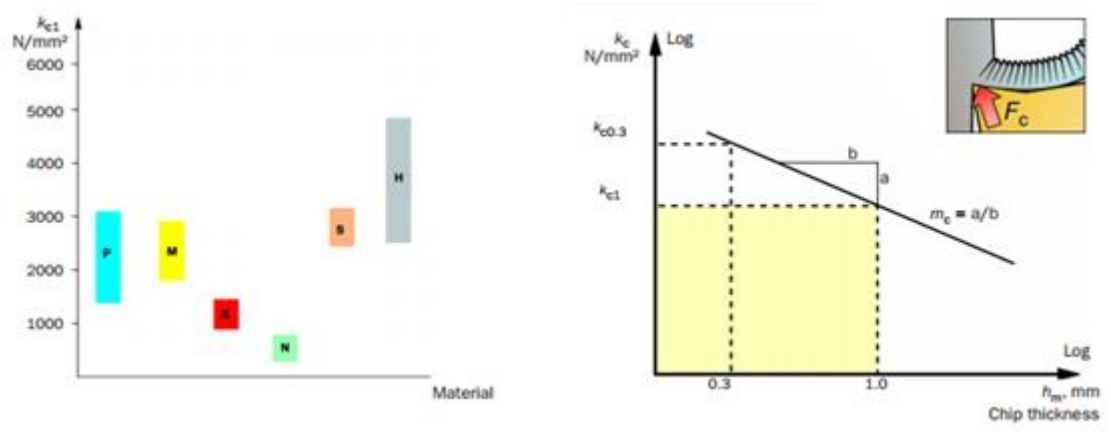

Figure 15: Specific cutting force depending on the material (ISO_Materials)

In machining, steel is the largest workpiece material used in the metal cutting area. It is an alloy with iron as the major component (Fe-based). The characteristics and the machinability of the product, differs depending on alloying elements, heat treatment and manufacturing process.

In our experimental tests, the material used is Stainless steel AISI 410.

Stainless steel has generally a low carbon content(C<=0,05%) and a chrome content higher than 12%. Various addition supply different characteristics such as resistance towards corrosion and strength at high temperatures. In general machinability decreases with higher alloy content. We are talking about a ferritic/martensitic material. Chips created are long and chip control is fair. The specific cutting force runs between 1800-2850 N/mm^2. This creates high cutting forces, built-up edge, heat and work-hardened surfaces while machining. (ISO_Materials)

MC code	Material group		Material sub-group		Manufacturing process		Heat treatment		nom	Specific cutting force, k_{c1} (lbs/inch²)	m_c
P5.0.Z.AN	5		0		Z		AN	annealed	200 HB	261,000	0.21
P5.0.Z.HT	5		0		Z	forged/rolled/cold/ drawn	HT	hardened+tempered	330 HB	333,500	0.21
P5.0.Z.PH	5	stainless steel ferritic/marten-sitic	0	main group	Z		PH	precipitation hard-ened	330 HB	406,000	0.21
P5.0.C.UT	5		0		C	cast	UT	untreated	250 HB	275,500	0.25
P5.0.C.HT	5		0		C		HT	hardened+tempered	330 HB	304,500	0.25
P5.1.Z.AN	5		1	free cutting steel	Z	forged/rolled/cold	AN	annealed	200 HB	239,250	0.21
M1.0.Z.AQ	1		0		Z	forged/rolled/cold drawn	AQ	annealed/quenched or annealed	200 HB	290,000	0.21
M1.0.Z.PH	1		0	main group	Z		PH	precipitation hard-ened	300 HB	348,000	0.21
M1.0.C.UT	1		0		C	cast	UT	untreated	200 HB	261,000	0.25
M1.1.Z.AQ	1	austenitic	1	machinability improved (as SANMAC)	Z		AQ		200 HB	290,000	0.21

Figure 16: Stainless Steel AISI 410 features (ISO_Materials)

2.8.Deflection

One of the biggest problems faced in turning processes is the elastic deformation of the tool or in the workpiece. This deformation is because of to the cutting forces resulting in the radial direction being different than expected or simply uncontrolled.

This elastic deflection has to be specially controlled when machining with long and slender tools. These tools are more likely to experience deflection because of its structure. The ratio length/diameter is a relation between length and diameter is used to describe the slenderness of the tool.

$$R_{L/D} = \frac{L}{D} \qquad (12)$$

In turning processes, the most important technical requirements refer to the dimensional accuracy and the finish surface quality of the produced part. This means that it is necessary to take control over the tool when it is experiencing this kind of elastic deflections. In order to accomplish it, the possible deflection that will suffer the tool has to be calculated. For this reason, a mathematical calculation needs to be carried out using the following equation:

Deflection (δ)

$$\delta = \frac{F_r \cdot L^3}{3 \cdot E \cdot I} \qquad (13)$$

F_r = Radial forces [N]

L = length of the unclamped part of the tool [mm]

E = Youngs' modulus [N/mm^2]

I = Moment of Inertia of the tool [mm^4]

Afterwards, this deflection needs to be corrected before the cutting operation is carried on for correcting this accuracy error.

A method developed by (Sørby & Sundseth, 2015) is proved to be very accurate when performing finishing turning with long boring bars, it is called the Three pass method. The method assumes that there is a linear, but not proportional relationship between the radial force and the cutting depth. As a summary, the method compensates the depth of cut for half of the deflection in the second cut and for the entire deflection in the third cut.

3. Turning model development

In machining, as it is assumed, there is a long list of possible errors that can reduce our cutting operation accuracy. Static deflections can lead to a nonconformity of the dimensional tolerance planned, or vibrations can lead to a poor surface finish, a shorter tool life or chipping of the tool.

In order to control those factors and manage the cutting operation in the desired way, a prediction of the cutting forces of the operation had to be carried on. These predictions are required to determine suitable machine tool and set up conditions for the operation. An engineering model is required for the operation, so vibrations and poor surface finish can be avoided.

As far as is known, mechanics and dynamics of cutting processes have not been precisely successful to predict the behaviour of a cutting operation without previous experimental tests in the same conditions as the desired operation.

The primary purpose of modelling cutting process is to elaborate a prediction of the cutting forces. With this knowledge not only these forces can be estimated, it can also help to estimate the power consumption, cutting tool properties and metal part quality. This model will help to optimize the cutting process parameters.

Cutting forces are defined by (Atabey, Lazoglu, & Y. Atlintas, 2002) as follows:

$$\begin{aligned} dFc &= dFtc + dFte = Ktc \cdot dA + Kte\, dLc \\ dFf &= dFfc + dFfe = Kfc \cdot dA + Kfe\, dLc \\ dFr &= dFrc + dFre = Krc \cdot dA + Kre\, dLc \end{aligned} \tag{13}$$

As the cutting force coefficients are mainly determined by cutting experiments, the most important part of the cutting process modelling is to model the metal shear force. This model includes two main features: the chip load modelling and the cutting force coefficients modelling.

The chip load model is determined by some parameters that are going to be explained in detail in the following paragraph. Briefly explained, these factors are: first, the uncut chip thickness and the width of cut, (in our situation the feedrate and the depth of cut) and second, our tool's geometry and the orientation of the tool and workpiece. In the other hand, the modelling of the cutting force coefficients will depend on the material properties of the workpiece and the cutting tool, the tool geometry, and the cutting speed.

3.1.1. Cutting coefficients

First of all, the cutting force coefficients are going to be introduced. As it has been explained, there is two ways of defining these force coefficients. The first one, is using the classical laws of cutting mechanics such as orthogonal to oblique cutting transformation proposed by (E.J.A.Armarego & R.C.Whitfield, 1985) and explained in detail in the point 2.3. And the second one is determining them mechanistically by conducting cutting test with the exact insert and curve fitting the force measurements against the chip geometry.

3.2.Chip load model

Cutting inserts characteristics are defined basically by the nose radius and can have uniform or irregular rake face. Moreover, chip thickness and therefore the cutting pressure amplitude and direction vary as a function of the nose radius, depth of cut, feed rate and side cutting angle. All this, heads to a complex and non-linear relation in which all these factors influence in the cutting force distribution and therefore, in the final result.

Moreover, the presence of static and dynamic deflection of the tool used for these operations must be considered. These deflections can lead to variations on the chip load distribution and cutting pressure. Hence, some of the operations such as internal turning with long and slender boring bars have to be exceptionally controlled.

Cutting forces are normally predicted as a function of uncut chip area that changes in a complex way depending on the nose radius and tool geometry. The cutting coefficients normally have to be obtained using mechanistic models and specially when the tool's geometry is irregular as a result of the chip breaking grooves and chip tool contact. These models are accomplished through a series of cutting tests where the specific tool is used at different cutting speeds, feedrate and depth of cut. The coefficients are evaluated by curve fitting the force expressions and chip geometry.

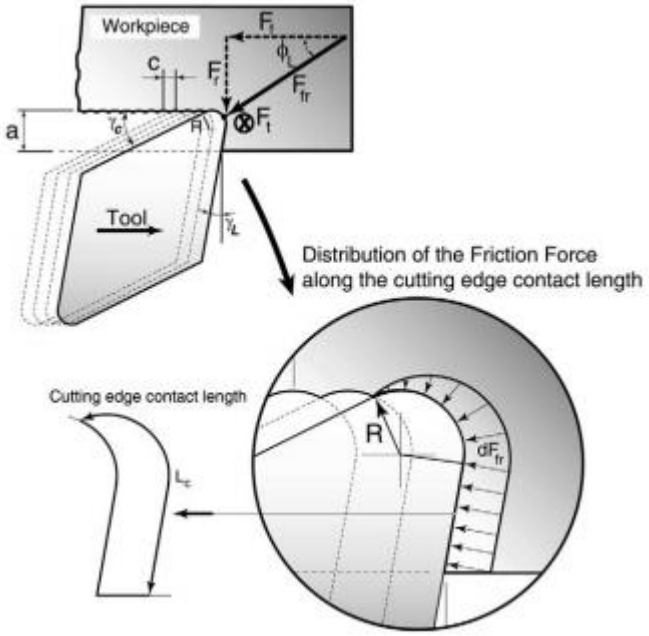

Figure 17: Friction Force distribution along the cutting edge (Atabey, Lazoglu, & Y. Atlintas, 2002)

In this part, the complex geometry of the formed chip is going to be modelled analytically with different cutting conditions and tool geometry. In order to accomplish it, a MATLAB programme has been created to define the actual dimension of the chip formed in each cut, depending on the characteristics named above. The cutting forces are modelled as friction and tangential cutting forces.

The friction force it's also divided in feed and radial force, the direction of total friction force is defined by the effective lead angle (ϕ_L), this angle is experimentally taken from the ratio

between these components (radial and feed). [For relatively large depths of cut, this angle tends to approach the side cutting angle of the insert]. The formulas is determined as follows (Atabey, Lazoglu, & Y. Atlintas, 2002),

$$\phi_L = arctan\frac{F_r}{F_f} \qquad (15)$$

The effective lead angle is obtained from the mechanistic modelled geometry of the chip and the tool. In the other hand, the cutting coefficients should be obtained as empirical functions of cutting speed, cutting edge contact length and uncut chip area.

Another possible way is the method proposed by (Armarego, 1993) and it has already explained in the previous chapter. This method consists in modelling the cutting pressure at each discrete oblique cutting edge element by applying the (E.J.A.Armarego & R.C.Whitfield, 1985) orthogonal to oblique transformation method. The forces are modelled using this method when the rake face of the tool is smooth. The method only requires the tool geometry, shear stress, shear angle and average friction coefficient of the orthogonal cutting process for specific work material.

3.3.Chip geometry program created

As it is shortly introduced in the last paragraph, a MATLAB programme has been created in order to predict the possible cutting forces that are going to be experienced during the cut. This programmed is based in the knowledge published by (Atabey, Lazoglu, & Y. Atlintas, 2002).

First of all, it has to be remarked that the fundamental geometry of a turning/boring insert is characterized by corner radius(R), side cutting edge angle (ψ) and end cutting edge angle(Ķ). Also, there are some characteristics that can affect the cutting mechanics, such as an irregular chip breaking and chip contact reduction grooves on the rake face of the tool.

The programme is going to calculate the chip area, and therefore the cutting force distribution. This distribution works as a function of depth of cut (Ap), feed rate (f) and side cutting angle (ψ). Different relative positions of the insert and configurations are being simulated as illustrated in the Fig.18 . It has to be noticed that the material left behind (uncut material) is also a function of the feed rate and nose radius, and is expected to be large when the feed rate is greater. This uncut material determines the surface finish quality, therefore all these parameters have been considered. The most common application in turning operations is when the feedrate is less than the nose radius of the insert.

This programme has considered a side cutting angle greater than 90 to work properly, this angle works as a variable for it. The uncut chip area formed is evaluated by the representation of three separate regions divided into small differential elements that are being calculated. The discrete summation of all these differential elements results into the total value of the uncut chip area. This summation is also distributed in the three different regions in order to keep the direction of the chip thickness that will represent the direction of the friction cutting force applied to each differential element (Atabey, Lazoglu, & Y. Atlintas, 2002). This force, as it is explained, will be divided in its two components, the feed force (acting in the x-axis of the representation) and the radial force (acting on the y-axe of the representation).

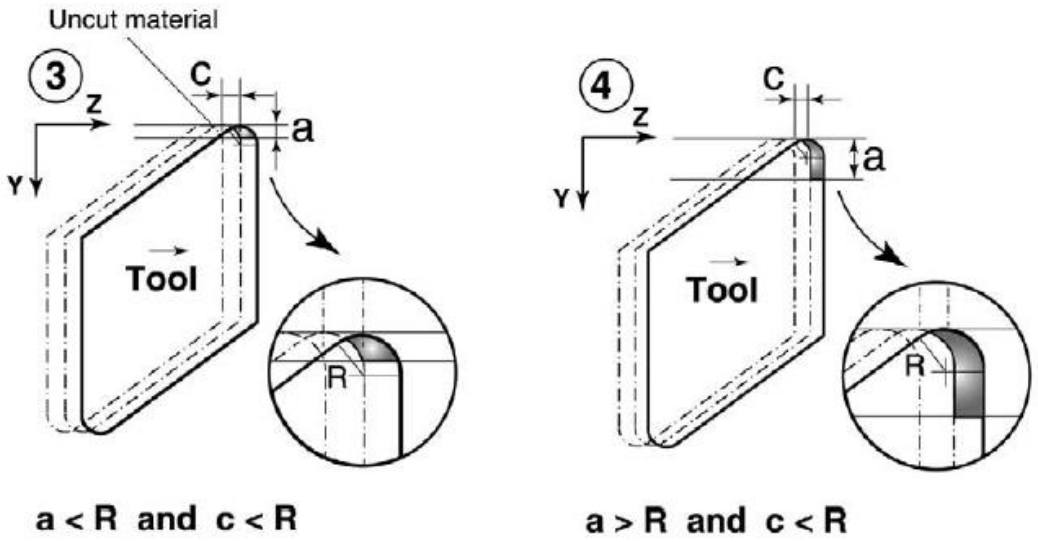

Figure 18: Configurations for the chip load programme (Atabey, Lazoglu, & Y. Atlintas, 2002)

In the following paragraph the calculation of the uncut chip area is explained in the three separated regions, assuming a configuration in where the depth of cut is greater than the nose radius. This configuration is needed to explain the three possible regions that are going to appear in the uncut chip area.

For Region 1 in Fig. 19 is shown that the uncut chip area is defined by two arcs with a radius equal to the nose radius (r_e) of the tool's insert. The centrum of these arcs is separated a distance equal to the feedrate(f or c in the figures).

The area of each differential element is approximated by calculating the summation of the differential rectangles included in that region. It is also shown that the region is extended below the 0˚ angle just the inclination of the side cutting angle (ψ or γ_L in the figures). The following expressions show the calculation method for these area:

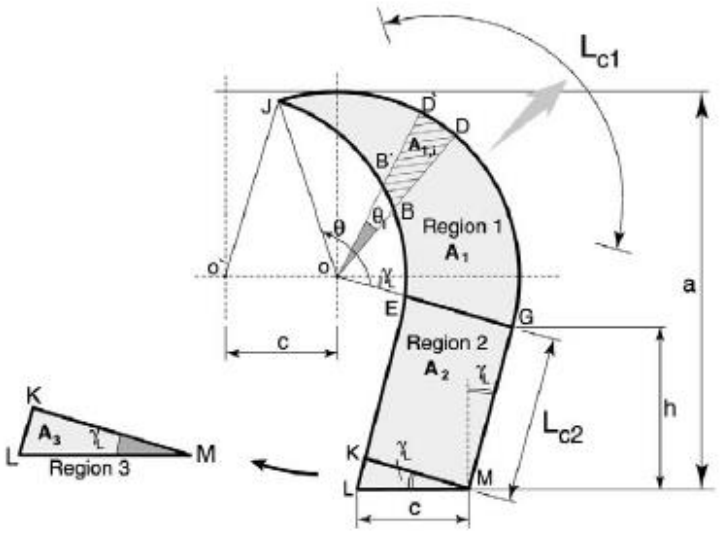

Figure 19: Uncut chip area configuration and definition of the regions (Atabey, Lazoglu, & Y. Atlintas, 2002)

Arc 1

$$\begin{aligned} x &= re * \cos(d\theta) \\ y &= re * sin\,(d\theta) \end{aligned} \qquad (16)$$

Arc 2

$$\begin{aligned} x &= re * \cos(d\theta) - c \\ y &= re * sin\,(d\theta) \end{aligned} \qquad (17)$$

3.3.1. Chip thickness

As far as it is known, the chip thickness distribution at each point along the chip load area and the cutting contact length is different and dependent on the tool geometry (R, γ_L, γ_c), feed rate (c) and radial depth of cut (a). The distribution of it along the cutting edge also varies.

It is assumed that the chip thickness is going to be the difference between these two arcs. This characteristic will also help to preserve the direction of the chip in all its differential elements in order to be able to divide the components in radial and feed direction.

The final equation for the calculation of the chip thickness is deduced by (Atabey, Lazoglu, & Y. Atlintas, 2002)as follows:

$$r = \sqrt{x^2 + y^2} \qquad (18)$$

Arc 1

$$r_1 = r_e \cdot \sqrt{\sin^2 d\theta + \cos^2 d\theta} \qquad r_1 = r_e \qquad (19)$$

Arc 2

$$r_2 = \sqrt{(r_e \cdot \cos d\theta - f)^2 + (r_e \cdot \sin d\theta)^2} \qquad (20)$$

Therefore, the difference will result in the Chip thickness (h):

$$h = r_e \cdot \sqrt{(r_e \cdot \cos d\theta)^2 - 2r_e f \cos d\theta + (f)^2 + (r_e \cdot \sin d\theta)^2} \qquad (21)$$

In the programme, the total chip area in Region 1 is evaluated by the discrete summation of all the differential elements. The differential elements have been considered as small rectangles with increments of 0,001. Area delimited as follows:

$$A_{1,i} = h \cdot 0{,}001 \qquad (22)$$

$$A_1 = \sum_{i=1}^{n} A_{1,i} \qquad (23)$$

Region 2

Although this is not the most accurate way to define region 2, it has been considered to be a rectangle. It is said that is not perfectly accurate due to the internal side (in the figure, side KE), it has a slight curvature induced by the corner radius of the previous tool position. Despite this knowledge, Region 2 is approximated by (Atabey, Lazoglu, & Y. Atlintas, 2002)as follows:

$$A_2 \cong |MG||KM| \qquad (24)$$

Finally, Region 3 is a simple triangle with an area calculated as:

$$A_3 = \frac{1}{2}|KM||LM| \sin \gamma_L \qquad (25)$$

With the 3 regions completely defined, the only thing left to get the entire Area is the summation of these 3 regions,

$$A = A_1 + A_2 + A_3 \quad (26)$$

The total cutting edge length in contact with the workpiece can also be calculated in this programme as the addition of the cutting edge length in Region 1 and Region 2.

$$Lc = L_{c1} - L_{c2} \quad (27)$$

Where L_{c1} is the discrete the contact length summation of the same number of differential elements (n) used for the calculation of the area in Region 1. Similarly, the contact length in Region 2 is equal to the length of *MG*.

As this programme shows, the entire chip area can be identified geometrically as a function of feedrate, depth of cut and geometrical characteristics of the tool such as the nose radius(r_e), the side cutting edge angle (γ_L) and end cutting edge angle (γ_c).

3.3.2. Modelling of cutting forces in the programme created

The cutting forces are represented by the tangential cutting force (Ft) and the friction cutting force (Ffr), that is resolved into the feed and the radial directions. In our programme, the differential cutting forces have been modelled as function of local chip area (dA), and the forces are represented by:

$$\begin{aligned} dF_t &= dF_{tc} = K_{tc} \cdot dA \\ dF_{fr} &= dF_{frc} = K_{frc} \cdot dA \end{aligned} \quad (28)$$

where dF_{tc},dF_{frc} are supplied by the removal of the chip and the cutting coefficients (K_{tc}, K_{frc}) used in it are dependent on the rake, inclination, chip flow angles, cutting conditions and work-tool material properties.

In our situation, they have been substracted of mechanistic experiments carried on in different studies. In these studies, the coefficients change inversely as functions of the uncut chip area(A), the cutting contact length (Lc) and the cutting speed(V_c). The relationship between them is non-linear due to the corner radius and the chip groove along the cutting edge. The variation of these coefficients represents the effects of the tool geometry on the cutting forces.

A decrease of these coefficients is associated to the reduction of the shear stress of the material and average friction coefficient at high speeds. As it known, the friction force acts perpendicular

to the cutting edge contact length and is proportional to the uncut chip Area of each differential element along the cutting edge.

3.3.3. Mechanistic modelling of cutting forces

The procedure carried on and, therefore, the programme generated is general and valid for different types of insert geometries and workpiece materials. One of the most important factors in the modelling of these forces is the effective lead angle. The effective lead angle () defines the direction of the total friction force, and is the angle generated between the friction and the feed direction (see Fig. 17). For relatively large depth of cut (above the nose radius), the effective lead angle tends to approach the side cutting angle (γ_L) of the insert, this generates a reduction of the F_r/F_f ratio. This angle can also be evaluated from each cutting test as follows:

$$\phi_L = \tan^{-1}\frac{F_r}{F_f} \qquad (29)$$

Our procedure has been evaluated with two different inserts (that are commented in the following section) with nose radius of 0.4 and 0.8 mm, and two different feed rates for each insert. The procedure consists in evaluating the forces in various operations with increasing depths of cut to evaluate the variation that these factors can generate in the programme and afterwards compare it with the real values taken from the experimental tests in the same conditions.

3.3.4. After experimental tests

As it is going to be explained in the next section of this project, and also it has been explained by (Atabey, Lazoglu, & Y. Atlintas, 2002), there are certain discrepancies between “measured” and “predicted” effective lead angles produced by the model created in this project. These differences are due to the fact that the friction force (F_f) may not be exactly acting in the same direction as the chip thickness, perpendicular to cutting edge.

In the paper, these discrepancies have been studied and an attempt of elaborating a relation between the actual effective lead direction and the predicted is performed. This investigation exposes that there are some important factors in the prediction of the real effective lead angle that have been overlooked. The effects of the cutting speed (V) and the cutting edge length (Lc) show a linear variation in the prediction of it. Therefore, the calculation of the angle can be adjusted by the addition of a simple modification factor (Km) that is also a linear function of Lc and V, and is presented by (Atabey, Lazoglu, & Y. Atlintas, 2002) as,

$$\phi_L = K_m(V, Lc)\phi_L{}^* \qquad (30)$$

In these equation, $\phi_L{}^*$ is the predicted effective lead angle based in the procedure elaborated in this project and ϕ_L is the new modified-predicted effective lead angle. The behaviour of this angle is different when acting above or below the nose radius, so two different modification factors are made by (Atabey, Lazoglu, & Y. Atlintas, 2002) as follows,

$$\begin{aligned} K_{m1} &= 1.0743 - 0{,}3567 \cdot 10^{-3} L_c + 0{,}9763 \cdot 10^{-4} V \quad for\ a < R \\ K_{m2} &= -0{,}0163 + 0{,}6299 L_c + 0{,}0013 V \quad for\ a \geq R \end{aligned} \qquad (31)$$

Where the cutting edge length is given in mm and the cutting speed in m/min.

These factors show a clear difference while working above and below the nose radius, this difference is mainly caused by the chip flow. When working below the nose radius (a<R), the effects of the cutting edge length and the cutting speed are almost negligible. In the other hand, they have a high relevance when the cutting operation is carried on in depths of cuts greater than the nose radius.

When working below the nose radius (a<R), the chip tries to find a way towards the centre of the corner radius. However, the chip is forced to flow away in the radial direction with friction forces continuously acting on it along the entire edge. These forces generate a curling chip.

These forces acting on the chip show a continuous increase along the edge contact length, reaching its highest point at the end of the cutting edge. This relationship is shown in the calculation of the modification factor K_{m2}. A graphic representation of these forces and the change generated with the predicted ideal friction force is represented in the Fig. []

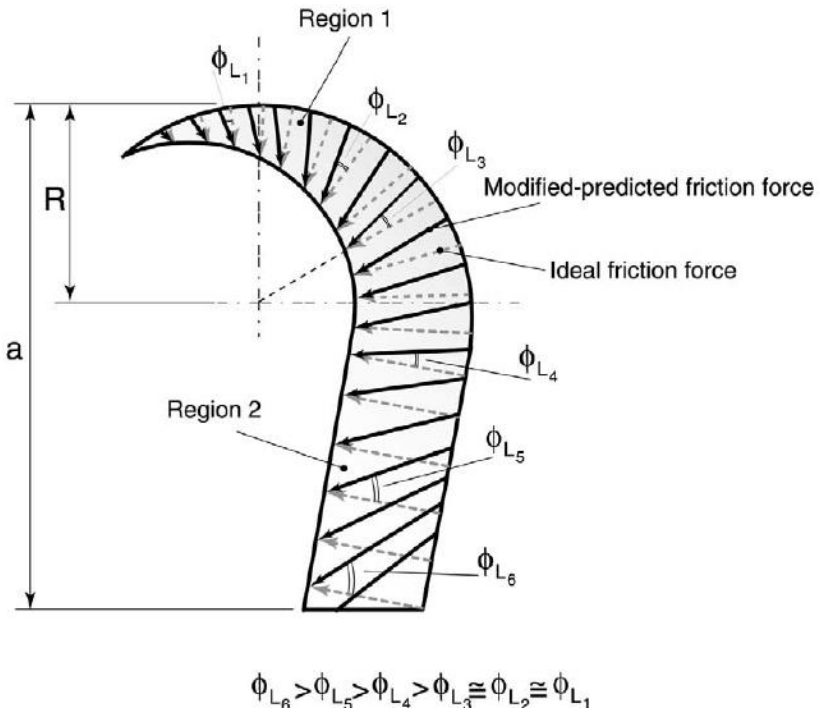

Figure 20: Deviation of the effective lead angle along the cutting edge contact length (Atabey, Lazoglu, & Y. Atlintas, 2002)

With these modified-predicted new model created, the radial and feed forces have to be recalculated. As both are function of the total friction force, the calculation is carried as follows,

$$F_r = F_{fr} \cdot \sin \phi_L$$
$$F_r = F_{fr} \cdot \cos \phi_L \qquad (32)$$

It should be noted that different tools or inserts characteristics will produce variations in the chip load model and cutting constants and accordingly, in the final forces.

Problems experienced in the application of these parameters

The creation of this programme has overcome through certain attempts of improving the calculations carried on in the method created by (Atabey, Lazoglu, & Y. Atlintas, 2002).

Finally, after several failed attempts, the programme is designed to predict the forces only as an ideal model. The idea of the correction of the effective lead angle presented by (Atabey, Lazoglu, & Y. Atlintas, 2002) is not working in all cutting operations, this method is only working for

depths of cut that generate a cutting edge contact length higher than 1,9556 mm. Fact that does not happen in any of the cutting operations that our test is designed for, considering that our range of depths of cut studied are 0-0.8 for the insert TNMG 16 04 04-MF and 0-1.2 for the insert TNMG 16 04 08-MM. However, the method was attempted to observe the results obtained from it and investigate another possible modification factor that fit with our experimental rank.

After several attempts of redesigning this modification factor, the model to establish a good and reliable relation between the forces in the radial and feed direction that can fit the real results of our cutting experiments, has not been solid enough. The modification of this factor only produces a stability in the values of the cutting operation performed above the nose radius and provokes the necessity of using a different coefficient than the one used in the other two simpler methods. Despite this, a graphical representation of the forces predicted in the radial direction is showed in the figure below.

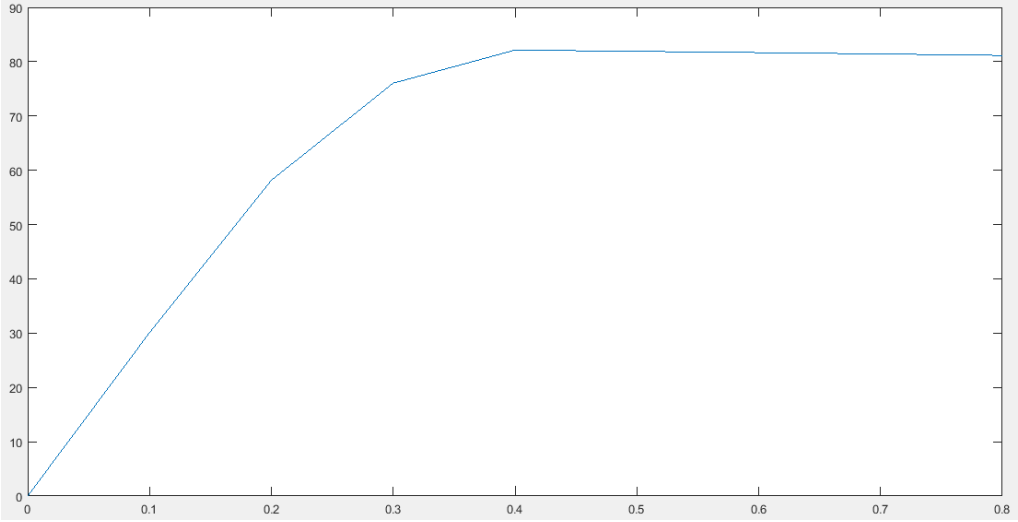

Figure 21: Graphical representation of the radial cutting force predicted with the new modification factor

Another point that should be discussed is the non-addition of the edge cutting length in the calculation of chip load model. Both models have been analysed.

On one hand, a model has been programmed with both relations, a constant coefficient for the Area's differential elements and another coefficient for the differential elements of the cutting edge length (see equation 33). In the other hand, another model that only includes the coefficient for the summation of the differential elements of the area has been designed too (see equation 34).

$$\mathrm{dFtc} = Ktc \cdot dA + Kte\, dLc \qquad \text{(Method 1) - (33)}$$

$$\mathrm{dFtc} = \mathrm{Ktc} \cdot \mathrm{dA} \qquad \text{(Method 2) - (34)}$$

The differences between these two methods have been studied and are shown with the representation of the radial forces predicted in both programmes for the characteristics of the insert TNMG 16 04 04-MF and a range on the depth of cut of 0 to 0,8 mm. As it has been explained, these results belong to the predicted ideal friction force component in the radial direction, therefore they will not be the exact values of the experimental tests.

DEPTH OF CUT (A_P)	RADIAL FORCE METHOD 1	RADIAL FORCE METHOD 2
0	0	0
0,1	29,705	28,744
0,2	56,879	55,981
0,3	74,053	73,283
0,4	79,883	79,167
0,5	79,532	78,821
0,6	79,195	78,490
0,7	78,858	78,158
0,8	78,522	77,826

Table 1: Numerical comparison of method 1 and 2

Method 1

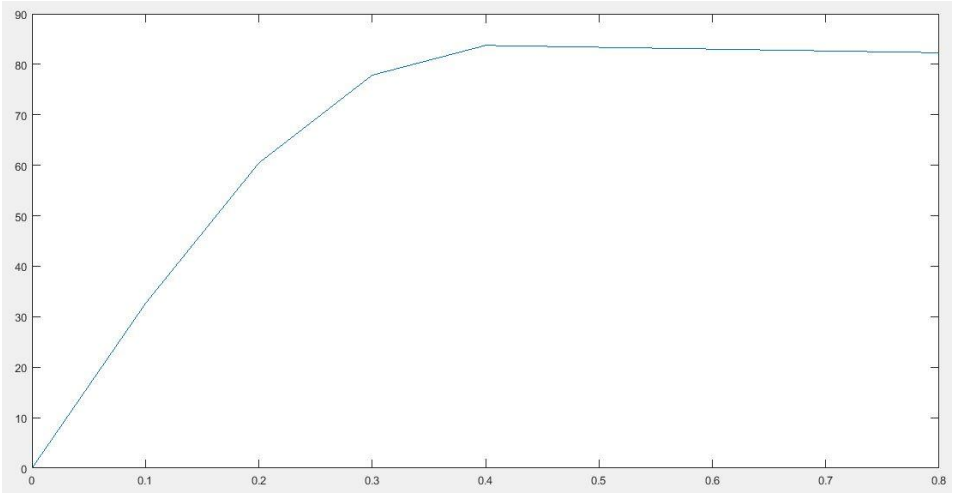

Figure 22: Graphical representation of method 1 for the insert TNMG 16 04 04-MF

Method 2

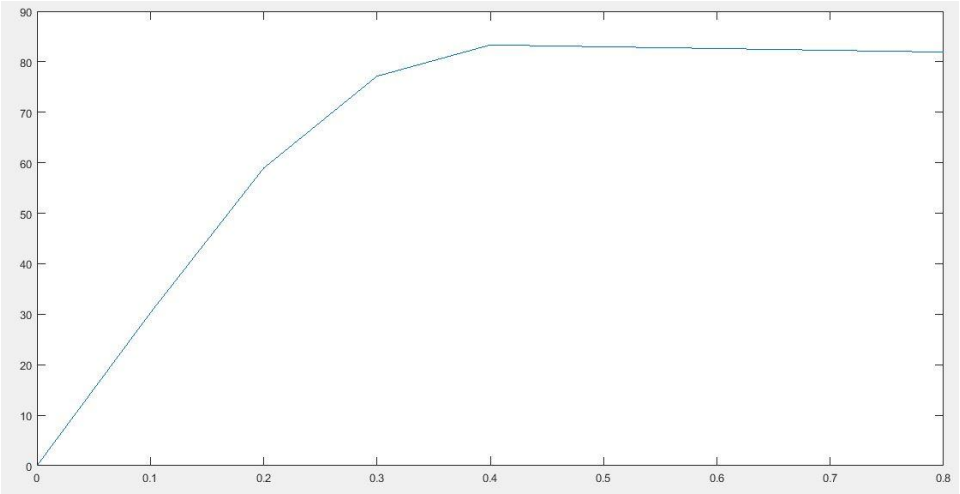

Figure 23: Graphical representation of method 2 for the insert TNMG 16 04 04-MF

As it can be seen, the differences between both models are certainly small and can even be considered negligible. For that reason, the simplest model has been chosen to represent the chip load model calculation method.

The effects of the contact edge length have been erased from the formula to determine the cutting forces in order to simplify as much as possible the method. This means that the equation (34) is the one used in the final programme. All of these factors have to be taken into account and, mainly, the fact that these values belong to an ideal model, which is not going to be the exact reality.

4. Experimental tests

In order to verify all the studies that have been carried out around the calculations and predictions of the cutting forces while turning, turning tests had been performed. These tests had been performed in a traditional lathe with the aggregate of a precise system of force measurement (Multicomponent dynamometer type 9257B) attached to the tool holder in order to study the forces received from the cutting operation in the different experiments carried on.

The cutting operations are performed in a workpiece of Stainless Steel AISI 410.

Figure 24: lathe Colchester 600 Grup MASTER 3250 used in the NTNU machining Laboratory

Figure 25: Workpiece for the experimental tests. Stainless Steel AISI 410

This measurement system, the Multicomponent dynamometer type 9257B, contain force dynamometers which help to divide the cutting forces in each of the three Cartesian directions (x,y,z). As it is explained before in this project, these three components represent the three forces suffered by the tool in each direction: Feed force (z), Tangential cutting Force (y) and Radial Force (x).

The dynamometer has a great rigidity and consequently a high natural frequency. Its high resolution can measure the smallest dynamic changes in large forces. It consists of four three-component force sensors located between a baseplate and a top plate. Each sensor contains three pairs of quartz plates, one sensitive to pressure in the z direction and the other two responding to shear in the x and y directions. (KISTLER)

Figure 26: Multicomponent dynamometer type 9257B

Figure 27: Charge amplifier type 5011

This system allows a precise method to obtain dynamic and quasistatic measurements of the three orthogonal force components practically without displacement. The range of values that the system is capable to register is from –5KN to 10 KN and the total dimension of the Top Plate attached to the lathe is 100x170 mm. More technical data about the measurement system can be found in the attachments.

4.1.Insert selection

These tests are performed as external turning, and the rigidity of the tool and the system in the conditions actual conditions of these operations, is assumed to be high. This means that the cutting operations performed are not suffering from detectable deflection, and vibrations are reduced to its minimum.

The tests are carried out with two different inserts. The inserts used for these operations are:

Inserts	*Nose radius* r_e	*Recommended depth of cut* a_p *(mm)*	*Recommended feed rate* f *(mm/rev)*
TNMG 16 04 04-MF	0,4	0,1 - 1,5	0,05 - 0,3
TNMG 16 04 08-MM	0,8	0,5 - 4,8	0,1 - 0,45

Table 2: Inserts recommended cutting configurations (SANDVIK Coromant, s.f.)

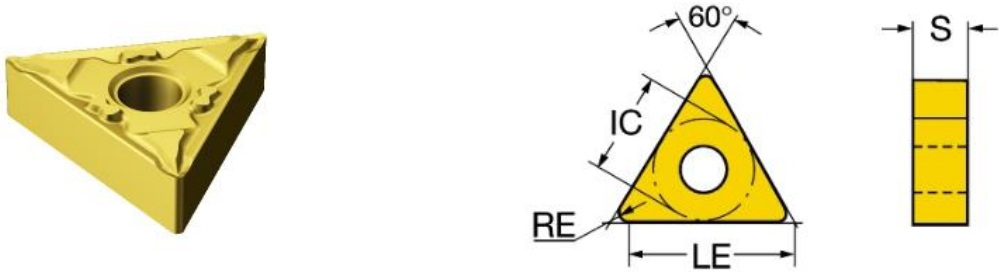

Figure 28: TNMG 16 04 04-MF insert geometry (SANDVIK Coromant, s.f.)

The two inserts used in the experimental tests have similar geometry and parameters, its main difference is the nose radius, 0.4 and 0.8mm. However, there is one characteristic that should be remarked, the purpose for what they are designed: MF means that is an insert produced to conduct finishing operations and MM is an insert designed for roughing operations. The precise characteristics of these inserts are found in the annexes.

The tool holder is also an important feature to mention due to its importance basically in the angle of attack of the insert into the workpiece. The side cutting edge angle is the most important parameter in it, in the figure is represented by KAPR and in our situation, it has a side cutting angle of 91˚ (SANDVIK Coromant, s.f.).

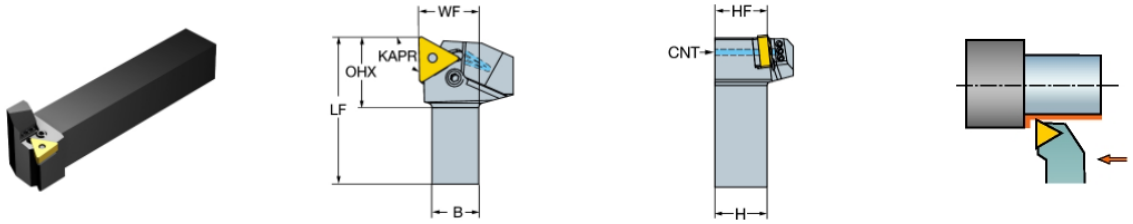

Figure 29: Tool holder for the inserts used

Tests carried out in the lathe are performed with growing depth of cut in order to study the relation of the forces acting in each point of the geometry of the insert. A few cuts are executed in each depth of cut, to assure the authenticity of the measure. The cut depths were

implemented in a range of values between 0.1 and 1 in the TNMG 16 04 04-MF insert with increments of 0.1 mm, and between 0.1 and 1.2 mm in the TNMG 16 04 08-MM insert.

It has to be considered that these operations with variations of depth of cut are carried on with the same feedrate. For the first bunch of cutting operations and the TNMG 16 04 04-MF insert, a feedrate of 0,1 mm/rev is selected.

These measurements concede a good overview of the forces obtained in these cutting conditions. The experimental tests have been also performed with two different feed rates in each insert to verify the influence of the feed rate in the cutting forces.

For the TNMG 16 04 04-MF insert the bunch of experiments with variation in Depth of cut were performed for a feedrate of 0,1mm/rev and 0,16mm/rev.

For the TNMG 16 04 08-MM insert, feed rates of 0,1 mm/rev and 0,2 mm/rev were selected.

All the tests were performed at a cutting speed of 200 m/min.

4.2.Results of the experimental analysis

The cutting operations performed can be described as stable processes and a suitable empirical representation of the theoretical background explained in this project. The repetition of these operations with different features can assure the authenticity of the results collected.

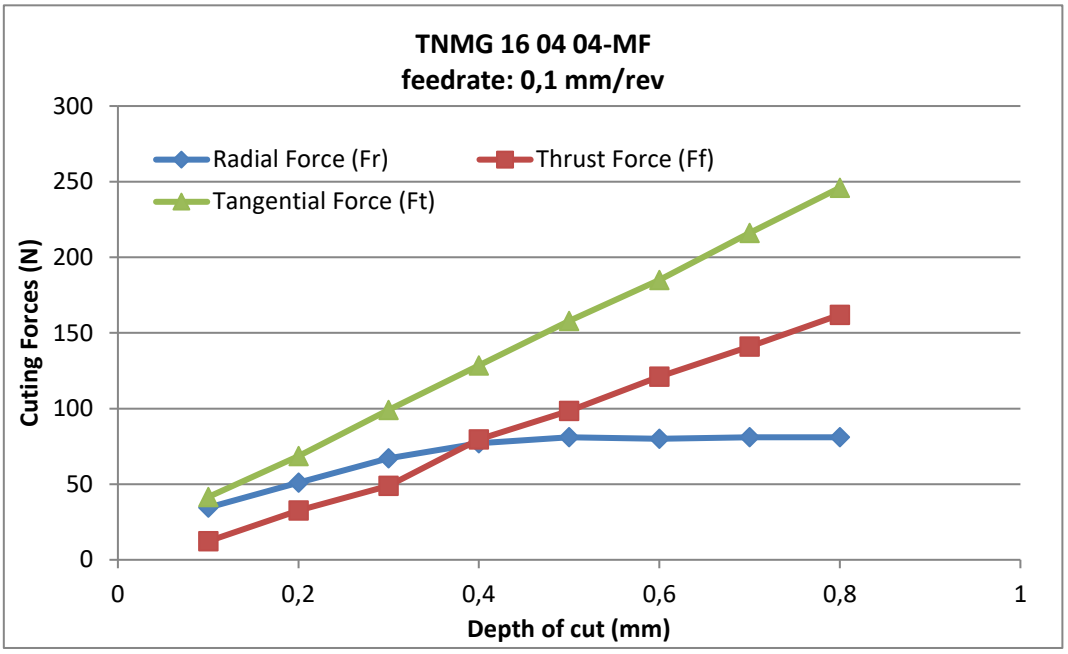

Figure 30: Graphical representations of the cutting forces measured in the insert TNMG 16 04 04-MF

In the figure, an example of the representation of the forces in the 3 cartesian axes is shown, the cutting parameters have been proved to worked as explained in the theoretical background. The experimental tests have been performed as explained in the last section, the graphical representation of all the results is included in the attachments.

In the graphical representations of the cutting forces, it can be clearly seen the constant growth of the tangential cutting force, directly related with the increment on the amount of material removed in each cut. This relation as the chip load model explains, is the main reason of the increment in all the cutting forces.

However, as it can be seen, in the cutting operations approaching a depth of cut similar to the nose radius, the uncertainty is highly increased. This uncertainty produces the moment when is more difficult to predict the cutting forces, as a result of the undefined direction of all the force vectors acting on the rounded surface. In the following figure, a basic representation of the direction in which these forces act is suggested.

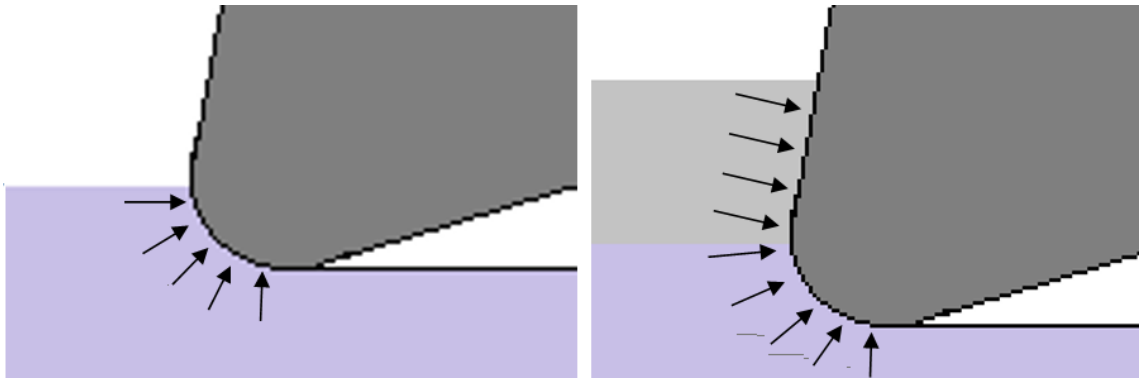

Figure 31: Representation of the direction of the forces received by the tool when machining below and above the nose radius.

In this point, is where the Thrust and Radial forces equalize its value. The redirection of the forces meets the same value while overtaking the nose radius, it's clearly represented in the figure above, and validated with the graphical representation of the experimental tests. Without taking into account any other parameter, this fact will happen with every configuration of feedrate, cutting speed or insert geometry.

After these moment and maintaining the increment in the depth of cut of the cutting operations, the Feed (Thrust) and the Radial forces will be clearly different. The Thrust force maintain his increment due to the portion of material removed, but the Radial force change drastically. This redirection of the forces produces a stabilization of the forces received in the radial direction. This situation is due to the redirection of the forces received in the tool, depending on the side cutting angle (ψ) of it, the forces will produce a little effect of pushing the tool in the opposite radial direction.

However, as it has been proved, this effect is the ideal model that is not perfectly represented in the real cutting operations, but it still produces the flattening of these forces. This effect causes the stabilization of the radial cutting forces received in the processes carried on above the nose radius.

4.3.Round insert experimental tests

In the experimental tests carried on in the NTNU laboratory, rounded inserts had been also tested in order to analyse the differences suffered in the three orthogonal directions and compare them with the normal inserts used in the main cutting tests.

These tests were performed in the same conditions as the rest of the cutting operations. A feed rate has been selected and the cutting operations has been conducted with increasing depth o cut.

Round inserts are used for cutting operations with difficult geometries and for the property of reducing the notch wear, a common problem which leads to an inferior quality. These inserts are made to perform in higher values of feed rate and speed to improve the productivity. The cutting edge contact length is increased and results in lower temperatures in the cutting edge.

The insert used is the RCMT 12 04 M0 235 and the tests are performed with a feed rate of 2,4 mm/rev, this feed rate is remarkably high if compared with the feed rates used in the rest of the insert. The recommended depth of cut for this insert is 3,00 mm (range of 1,20 – 4,80) and the recommended feed rate is 0,60 mm/rev (range of 0,12 -1,20).

The experimental test results are as follows,

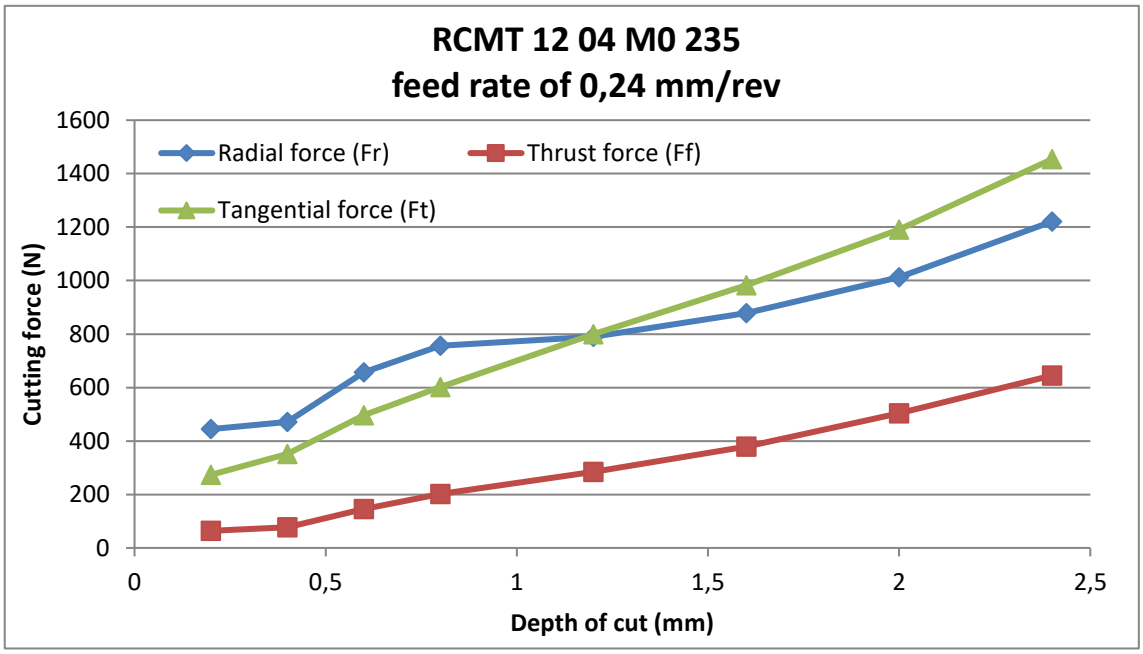

Figure 32: Graphical representation of the cutting forces with the insert RCMT 12 04 M0 235

As it can be seen, these inserts can have really good properties in the characteristics named before, but the forces experienced when machining with them are particularly high. In rigid system where these forces don't generate unstable processes, these inserts are useful for accelerating the productivity without influencing the quality. However, if the cutting operation

is performed in a system with poor rigidity or if a boring operation is needed, these inserts generate forces exceptionally high that can lead into high deflections or vibrations.

5. Relation between predicted and measured Radial forces

In these section, a comparison of the predicted cutting forces developed by the MATLAB programme created and the forces measured in the experimental tests carried out in the NTNU laboratory is carried out. In particular, the force studied and the one that is going to be deeply discussed is the Radial force (Fr), cause is the force that can provoke vibrations and possible deflection, generating a bad result in the finish quality or in the dimension accuracy of the workpiece.

As it has been explained, the MATLAB programme created can represent the ideal friction force. This situation is going to be discussed to analyse the differences that generate the variation of the effective lead angle in the final results that are going to be represented.

A graphical representation of the predicted radial force and the measured radial force for each condition is presented. The parameters that have to be considered before running the programme are the side cutting edge angle, the nose radius of the insert and the feed rate.

Four different situations are presented: two different tools have been used and each experimental cutting sequence has been performed with two different feed rates.

5.1.TNMG 16 04 04-MF

First the graphical relation between the measured and predicted forces of the TNMG 16 04 04-MF insert are presented. This insert presents a nose radius of 0,4 mm and a side cutting angle of 91˚. The first figure shows the graphical representation of this relation for a feed rate of 0,1 mm/rev and the second one for 0,2mm/rev.

For this insert and workpiece material, the cutting coefficient evaluated in the cutting experiments is 1900. It has been used for both sequences in order to have a clear relation of the changes experimented in the prediction programme with the change of the feed rate in the

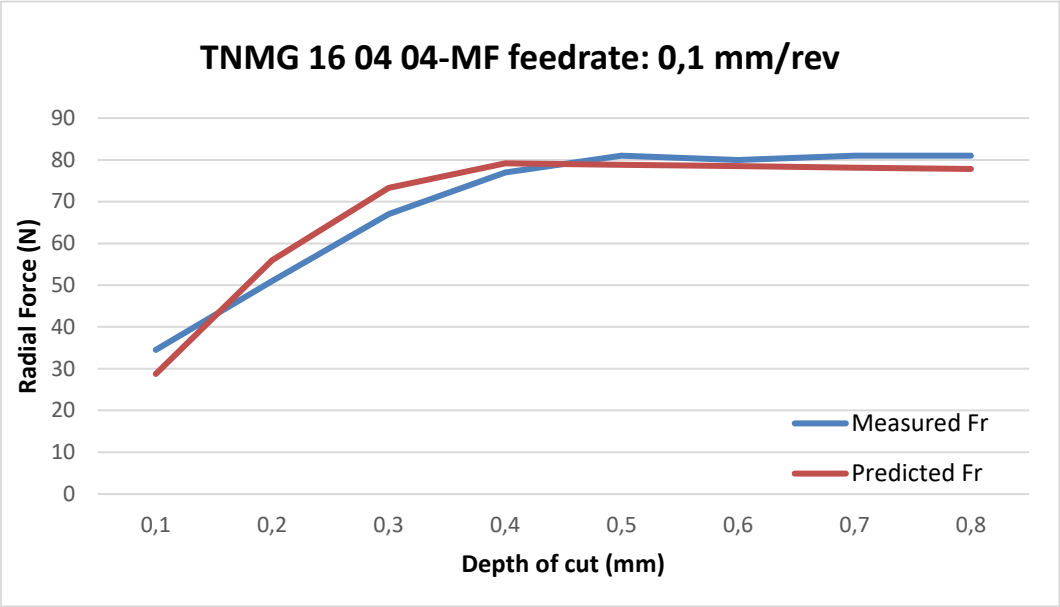

Figure 33: Predicted vs Measured Radial forces in the insert TNMG 16 04 04-MF with a feed rate of 0,1 mm/rev

same insert.

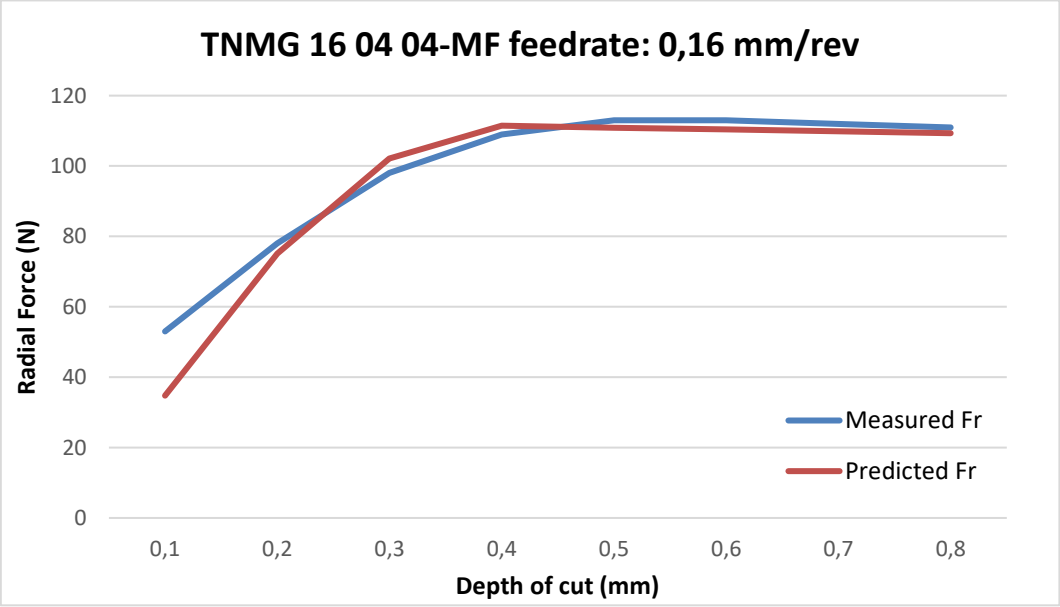

Figure 34:Predicted vs Measured Radial forces in the insert TNMG 16 04 04-MF with a feed rate of 0,16 mm/rev

Both representations fit with the curves drawn by the measured values taken from the experimental tests. But there are some points that should be mentioned in order to understand completely the relation presented in these graphics.

First of all, it has to be mentioned that in the moment when the increasing depth of cut reaches the value of the nose radius, is the moment of most uncertainty, that means that the measured values in the different experimental tests can have big differences between each other.

One of the most important facts that it is demonstrated in the graphical representation is the fact that in the point when the increasing depth of cut overtakes the nose radius, the predicted and measured curve reach a similar value. After this point, clear differences are revealed. The model created represents an ideal situation and show decreasing radial forces and, in the other hand, the measured results show, that these forces get stabilized but don't get a decreasing behaviour.

This fact has already been explained and it is due to the difference between the ideal predicted effective lead angle and the real one experienced by the friction force. This variation in the effective lead angle also generates the difference between the measured and predicted force when the depth of cut is small.

A factor that should not be forgotten is that this insert is a finishing insert (MF), this feature means that the cutting edge is sharper than the normal inserts used for roughing but also its cutting edge strength is also reduced. This characteristic provides a better finish surface quality and accurate results and; as it is shown in these representations, it also produces more easily predictable and accurate results when a prediction of the cutting forces is needed.

5.2.TNMG 16 04 08-MM

The experimental cutting operations were also performed with another insert, the insert TNMG 16 04 08-MM, and a graphical relation between the predicted and measured Radial forces with this insert is also presented. The two figures represent the graphical representation of them with a feed rate of 0,1 mm/rev and the second one with 0,2 mm/rev. This insert has a similar geometry as the first insert used in the experimental tests, it is provided with a side cutting angle of 91˚, the main difference with the other insert is the nose radius, that in this situation is 0,8 mm.

For these insert another strategy had to be carried out. The usage of the same coefficient cannot be used for both feed rates, and different cutting coefficients of C_1=2800 for the first configuration and C_2=2400 for the second configuration were needed. The fact that the same

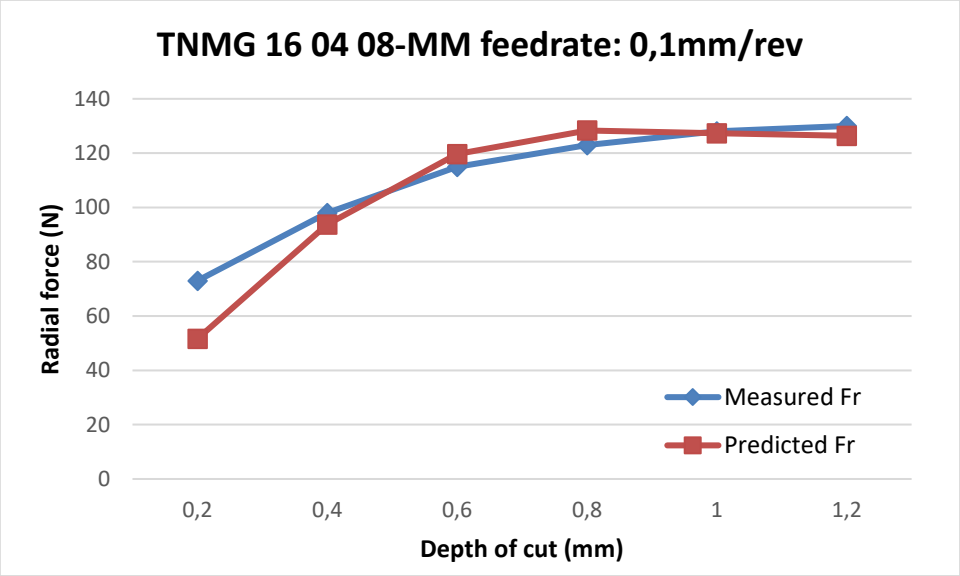

Figure 36:Predicted vs Measured Radial forces in the insert TNMG 16 04 08-MM with a feed rate of 0,1 mm/rev

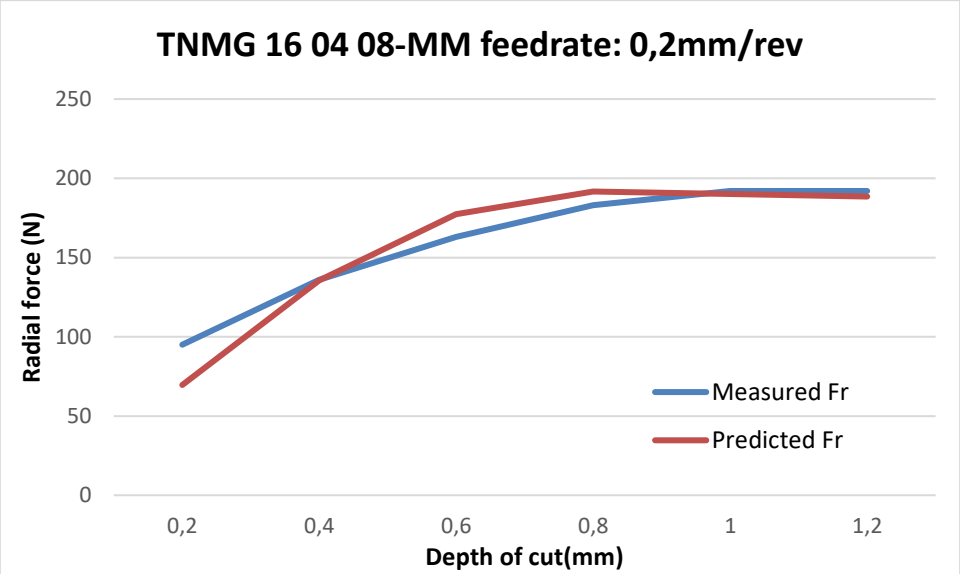

Figure 35:Predicted vs Measured Radial forces in the insert TNMG 16 04 08-MM with a feed rate of 0,2 mm/rev

relation cannot work with both configurations has been analysed.

The main characteristics that can produce these changes are the own cutting insert parameters and the procedure used to programme the prediction of the forces.

First, the insert used in this situation is a roughing insert (MM). This fact means that the inserts cutting edge is not as sharp as the first used and the results are not supposed to have the same

accuracy. Moreover, it also means that this cutting edge strength is higher in order to support greater depths of cut. This fact can affect in a certain way to our experimental data.

In the other hand, it has to be highlighted that the programme created to elaborate the prediction of the cutting forces has a strong dependency on the feed rate. This means that the feed rate affects considerably in the distribution of the chip load area while the effect of the nose radius doesn't affect in it with the same magnitude.

After the obtainment of the different coefficients for each configuration of the cutting operations, the graphical representation of the measured and predicted curved is performed.

Similar conclusions as those taken for the other insert are obtained, the predicted curves drawn fit the measured experimental curves. It can also be observed that when the nose radius is reached, the same point of uncertainty is found, and the curves cross following its own behaviour. The predicted curve tends to slightly decrease and the measured curve starts to stabilize, as it has been explained, because of the different projection of the effective lead angle (ϕ_L).

As a conclusion taken mainly in the differences that can be seen while predicting the forces in this insert, the MATLAB programme is not a perfect tool for evaluating all the possible variables that can modify the radial cutting force. It needs to be improved, to establish a more suitable relation between all the tool's geometrical parameters and the cutting configuration influencing in the prediction. An improvement to make the programme not so related on the feed rate and, consequently find a more accurate coefficient to perform a better prediction on the cutting operations desired. In summary, to make it capable of being a solid tool in the prediction of the cutting forces.

6. Deflection prediction SILENT TOOL boring bar

In order to compare the results of the tests performed in the NTNU laboratory with the tests performed in SANDVIK, a calculation of the deflection that each depth of cut can produce when machining in internal turning with a SILENT TOOL boring bar has been carried out. It must be considered that, when radial forces act in this kind of tool, it causes a deflection that at the same time makes the real depth of cut to be less than programmed, therefore the forces will be lower too.

In order to establish the desired relationship, the real characteristics of SILENT TOOL boring bar have been taken in the prediction, and the equation (13) explained in the deflection section have been used.

Unclamped length = 320 mm

Diameter= 40 mm

Young's modulus = 210 GPa

Figure 37: Silent Tools Boring bar (SANDVIK Coromant, s.f.)

With the characteristics of the boring bar, the calculation of the deflections for the insert TNMG 16 04 04-MF is represented in the following figure. This representation shows that the deflection related to the increasing depth of cut has the same relation than the graphical representation of the radial force as it can be checked in the Fig.33. This property is easily explained by the equation(13) of the deflection. In the Fig. 38, the deflection of this insert with a feed rate of 0,1 mm/rev is shown, the representation of the same calculations with different inserts and feed rates can be found in the attachments.

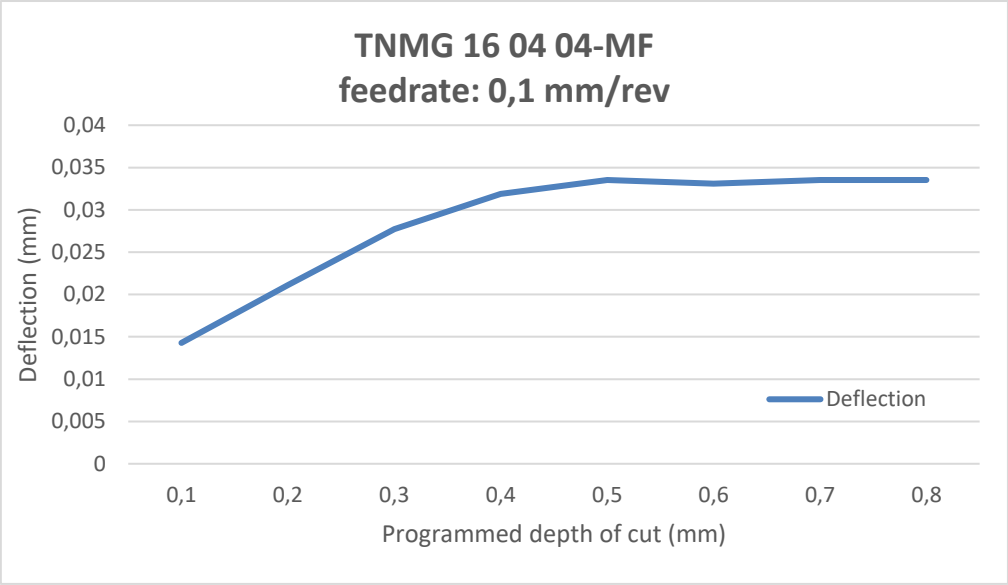

Figure 38: Graphical representation of the deflection, the TNMG 16 04 04-MF insert is used.

As the cutting depth keep increasing but still performs below the nose radius, the forces act strongly in the radial direction pushing the tool away from the workpiece. Therefore, in a boring operation, the deflection suffered by the tool will be high and raising while increasing the depth of cut. As the depth of cut continue to increase, and exceed the nose radius, part of these forces will change direction due to the angle of attack with the insert. The forces above the nose radius can help to push the tool in the opposite direction in the radial axe and lead to a minor deflection. These explanation is according to the ideal model of friction forces that, after the experimental tests carried out is proved not to be the exact performance of the cutting forces. However, it has to be mentioned that the forces change drastically his direction after overtaking the nose radius, causing a flattening on the radial forces received.

In this moment, with the calculated deflection, the real depth of cut can be shown as follows,

$$Real\ Ap = Programmed\ Ap - Deflection \qquad (35)$$

Then, the relation between real and programmed depth of cut can be plotted. A linear relationship can be clearly observed between them as it can be seen in the following figure. This relationship can be verified with the graphical representation of it with the other insert and different feed rates, that can be found in the attachments.

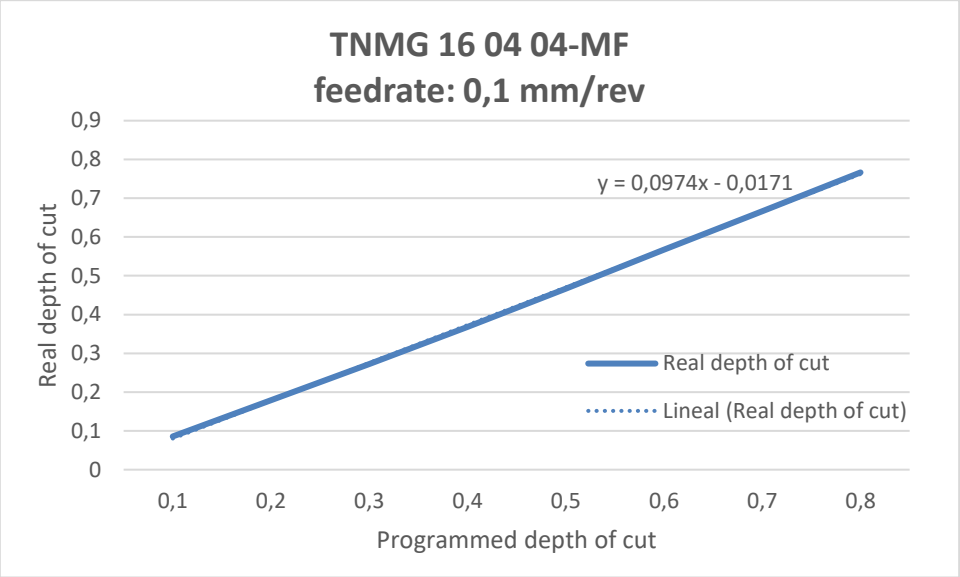

Figure 39: Graphical representation of Real A_p vs Programmed A_p

This relation is an important finding in the prediction of the real depths of cut that a cutting operation with a boring bar can achieve. An interesting characteristic is that with different deflections, experiencing a big variation if the cutting operation is being performed below or above the nose radius, a completely linear relation is achieved in the prediction of the real depth of cut.

More experimental tests have to be carried on to verify the authenticity of a finding of these characteristics, cause it can be used to establish a method of automatization in cutting operations with boring bars.

7. Conclusions

After the studies performed to understand the influence of the cutting tools geometry and the cutting parameters on the cutting forces, a clear goal is found to be the purpose of the project. The creation of a model to predict the cutting forces acting on the machining tool is needed to avoid and correct potential errors in the cutting operations.

For this reason a MATLAB programme is designed, this programme generates a prediction of the chip load area to analyse the forces depending on tool's geometry and cutting conditions. Different variants had been tested to find a model to predict the cutting forces. Moreover, experimental tests had been performed to analyse and compare the result with the predicted forces.

The relation between the predicted and the experimental results is made by graphical representation of the radial force values. This representation shows clearly that, after getting the cutting coefficient through the empirical cutting tests, an approximate prediction of the radial force is made by the programme created. The prediction draws a curve with the same tendency but not the exact behaviour. These little differences are generated by the effective lead angle (). This angle is found to be described by an ideal friction force in the programme created, and leads in a variation of the direction of the forces. This factor generates, for example, the redirection of the forces when the depth of cut is greater than the nose radius, simulating a reduction of the radial force due to the pushing of these forces in the opposite direction. These variations can be observed in all the configurations (tool/cutting conditions) performed in the experimental tests.

Several modification factors have been attempted in order to correct this angle and simulate a more accurate direction of the forces, but the modification still has to be improved.

In the other hand, other differences have been seen in the TNMG 08 insert. In this insert, a different cutting coefficient has had to be found for the variation of feed rate between the tests. These fact can be influenced by different parameters. First, this insert is a roughing insert, the results taken from it can not be that accurate. However, the main issue is in the programme created, it has a strong dependency in the feed rate stablished for the operation and is not that influenced by the nose radius of the tool.

As a conclusion the MATLAB programme is not a perfect tool for evaluating all the possible variables that can modify the radial cutting force. It needs to be improved, to establish a more suitable relation, to make it capable of being a solid tool in the prediction of the cutting forces.

As a final proposal, the prediction of Silent Tool's boring bar deflection has been calculated with the values of the experimental tests performed. With this delfection the real depth of cut produced can be calculated. There is a linear and suitable relationship between the real and the programmed depth of cut.

8. Bibliography

Altintas, Y. (2012). *Manufacturing Automation, Second Edition.* Cambridge University Press.

Armarego, E. (1993). *Material removal processes.*

Atabey, F., Lazoglu, I., & Y. Atlintas. (2002). Mechanics of boring processes. *International Journal of Machine Tools & Manufacture*, 463-476.

CADEM NCyclopedia multimedia. (n.d.). Retrieved from http://cadem.com

E.J.A.Armarego, & R.C.Whitfield. (1985). Computer Based Modelling of Popular Machining Operations for Force and Power Prediction.

E.J.A.ArmaregoV.KarriA.J.R.Smith. (1993). *Computer-Aided Predictive Models for Fundamental Rotary Tool Cutting Processes.*

Eynan, M., & Altintas, Y. (2009). Chatter Stability of General turnig operations.

Groover, M. (2011). *Principles of modern manufacturing.*

ISO_Materials. (n.d.). SANDVIK Coromant.

KISTLER. (n.d.). Multicomponent dynamometer type 9257B.

Mecholic. (n.d.). Retrieved from http://www.mecholic.com

Merchant, M. (1945). *Mechanics of metal cutting process.*

Mitsubishi Materials Corporation. (n.d.). Retrieved from http://www.mitsubishicarbide.com

Polini, W., & Prisco, U. (2002). The estimation of the diameter error in bar turning: a comparison.

Sadílek, M., Dubsk´y, J., Sadílková, Z., & Poruba, Z. (2015). Cutting forces during turning with variabledepth of cut.

SANDVIK Coromant. (n.d.). Retrieved from https://www.sandvik.coromant.com

Sørby, K., & Sundseth, E. (2015). High-accuracy turning with slender boring bars. 6.

Stephenson, D. A., & Bandyopadhyay, P. (1997). Process-Independent Force Characterization for Metal-Cutting Simulation.

10. Annexes

10.1. First and definitive MATLAB Programme created. Method 1 applied. Equation(33)

In the MATLAB code, only the feed rate and the geometric variables related to the insert of the cutting tool have to be introduced. In this variables it is also found the cutting coefficient for the specific cutting operation. This fact works with the three different codes.

```
function [Fy] = plotproba( Ap )      %Fy      represents      the      radial      force
%UNTITLED2        Summary        of        this        function        goes        here
%                              Detailed          explanation          goes          here
r     =     0.4;                                                    %Nose     radius
f     =     0.1;                                                      %Feed     rate
Ap;                                                                 %Depth    of    cut
th    =    -0.0174533;         %Radians    for    our    side    cutting    angle    91    degrees
h=r-sqrt((r*cos(th))^2-2*r*f*cos(th)+f^2+(r*sin(th))^2);
F1x=0;
F1y=0;
A1=0;
at2=0;
A2=0;
A3=0;
F2x=0;
F2y=0;
F3x=0;
F3y=0;
Y=r+r*sin(-th);
s=0;
k=1900;
f3=f;
t=f*sin(-th);

%Region                                                                          2
if                                                                             Ap>Y
    d=Ap-Y;
    Lc2=d/cos(th);
    A2=Lc2*f*cos(th);
    while                                                                      s<=Lc2
        a2=f*cos(th)*0.001;
        Ft2=a2*k;
        at2=at2+a2;
        fx2=Ft2*cos(th);
        fy2=Ft2*sin(th);
        F2x=F2x+fx2;
        F2y=F2y+fy2;
        s=s+0.001;
    end
end

%Region3
if                                                                             Ap>Y
    if                                                                          t>0
        ht=f3*cos(th);
```

```
        a3=ht*0.001;
        Ft3=a3*k;
        A3=A3+a3;
        f3x=Ft3*cos(th);
        f3y=Ft3*sin(th);
        F3x=F3x+f3x;
        F3y=F3y+f3y;
    end
    t=t-0.001;
    f3=t/sin(-th);
end
%Region                                                              1
if                                                                  Ap>Y
    while                                                           h>=0
        h=r-sqrt((r*cos(th))^2-2*r*f*cos(th)+f^2+(r*sin(th))^2);
        if                                                          h>=0
            a=h*0.001;
            Ft1=a*k;
            hx=Ft1*cos(th);
            hy=Ft1*sin(th);
            F1x=F1x+hx;
            F1y=F1y+hy;
            A1=A1+a;
        end
        th=th+0.001;
    end
else
    alpha=asin((r-Ap)/r);                          %New   angle   for   a   Ap<r
    while                                                           h>=0
        h=r-sqrt((r*cos(alpha))^2-2*r*f*cos(alpha)+f^2+(r*sin(alpha))^2);
           if                                                       h>=0
               a=h*0.001;
               Ft1=a*k;
               A1=A1+a;
               hx=Ft1*cos(alpha);
               hy=Ft1*sin(alpha);
               F1x=F1x+hx;
               F1y=F1y+hy;
           else
               break
           end
        alpha=alpha+0.001;
    end
end
%Sumation                                  of                                forces
Fx=F1x+F2x+F3x;
Fy=F1y+F2y+F3y;
A=A1+A2+A3;
end
```

10.2. MATLAB Programme corresponding to the Method 2. Addition of the effects of the cutting edge length. Equation(34)

The variables explained in the last section along with the cutting coefficients have to be introduced.

```
function [Fy] = plotprobaamblc( Ap )
%UNTITLED2 Summary of this function goes here
% Detailed explanation goes here
r = 0.4; %Nose radius
f = 0.1; %Feed rate
Ap; %Depth of cut
th = -0.0174533; %Radians for our side cutting angle 91 degrees
h=r-sqrt((r*cos(th))^2-2*r*f*cos(th)+f^2+(r*sin(th))^2);
F1x=0;
F1y=0;
A1=0;
at2=0;
A3=0;
A2=0;
F2x=0;
F2y=0;
F3x=0;
F3y=0;
Y=r+r*sin(-th);
s=0;
k=1850;
f3=f;
t=f*sin(-th);
alpha=asin((r-Ap)/r);
alpha1=alpha;
kl=8;
Lc=0;
Lc2=0;
%Region 2
if Ap>Y
    d=Ap-Y;
    Lc2=d/cos(th);
    A2=Lc2*f*cos(th);
    while s<=Lc2
        a2=f*cos(th)*0.001;
        Ft2=a2*k;
        at2=at2+a2;
        Fl2=0.001*kl;
        fx2=(Ft2+Fl2)*cos(th);
        fy2=(Ft2+Fl2)*sin(th);
        F2x=F2x+fx2;
        F2y=F2y+fy2;
        s=s+0.001;
    end
end

%Region3
if Ap>Y
    if t>0
```

```
        ht=f3*cos(th);
        a3=ht*0.001;
        Ft3=a3*k;
        A3=A3+a3;
        f3x=Ft3*cos(th);
        f3y=Ft3*sin(th);
        F3x=F3x+f3x;
        F3y=F3y+f3y;
    end
    t=t-0.001;
    f3=t/sin(-th);
end
%Region                                                                  1
if                                                                      Ap>Y
    while                                                               h>=0
        h=r-sqrt((r*cos(th))^2-2*r*f*cos(th)+f^2+(r*sin(th))^2);
        if                                                              h>=0
            a=h*0.001;                          %In differential of area, we use 0.001
            Ft1=a*k;
            Fl1=0.001*r*kl;                    %In lc, we use differential of r*0.001
            hx=(Ft1+Fl1)*cos(th);
            hy=(Ft1+Fl1)*sin(th);
            F1x=F1x+hx;
            F1y=F1y+hy;
            A1=A1+a;
        end
        th=th+0.001;
    end
    Lc1=th*r+(0.0174533)*r;
else

        alpha=asin((r-Ap)/r);                          %New angle for a Ap<r
        while                                                           h>=0
            h=r-sqrt((r*cos(alpha))^2-2*r*f*cos(alpha)+f^2+(r*sin(alpha))^2);
            if                                                          h>0
                a=h*0.001;
                Ft1=a*k;
                A1=A1+a;
                Fl1=0.001*r*kl;
                hx=(Ft1+Fl1)*cos(alpha);
                hy=(Ft1+Fl1)*sin(alpha);
                F1x=F1x+hx;
                F1y=F1y+hy;
            else
               break
            end
         alpha=alpha+0.001;
        end
    Lc1=(alpha*r)-(alpha1*r);
end
%Sumation                                  of                                forces
Fx=F1x+F2x+F3x;
Fy=F1y+F2y+F3y;
A=A1+A2+A3;
Lc=Lc1+Lc2;
end
```

10.3. MATLAB Programme corresponding to the Method with the modification factor applied.

```
function [Fy] = plotultimaproba( Ap )
%UNTITLED2 Summary of this function goes here
% Detailed explanation goes here
r = 0.4; %Nose radius
f = 0.1; %Feed rate
Ap; %Depth of cut
th = -0.0174533; %Radians for our side cutting angle 91 degrees
h=r-sqrt((r*cos(th))^2-2*r*f*cos(th)+f^2+(r*sin(th))^2);
F1x=0;
F1y=0;
A1=0;
at2=0;
A3=0;
F2x=0;
F2y=0;
F3x=0;
F3y=0;
Y=r+r*sin(-th);
s=0;
k=1800;
f3=f;
t=f*sin(-th);
alpha=asin((r-Ap)/r);
alpha1=alpha;
kl=10;
th2=th;
Lc2=0;
V=200;

%Region 1
if Ap>Y
    while h>=0
        h=r-sqrt((r*cos(th))^2-2*r*f*cos(th)+f^2+(r*sin(th))^2);
        if h>=0
            a=h*0.001;
            Ft1=a*k;
            Fl1=0.001*r*kl;
            hx=(Ft1+Fl1)*cos(th*1.0743); %Theory of km1 in the paper.(Lc & V
negligible)
            hy=(Ft1+Fl1)*sin(th*1.0743);
            F1x=F1x+hx;
            F1y=F1y+hy;
            A1=A1+a;
        end
        th=th+0.001;
    end
    Lc1=th*r+(0.0174533)*r;
else

        alpha=asin((r-Ap)/r); %New angle for a Ap<r
        while h>=0
```

```
            h=r-sqrt((r*cos(alpha))^2-2*r*f*cos(alpha)+f^2+(r*sin(alpha))^2);
            if                                                          h>0
                a=h*0.001;
                Ft1=a*k;
                A1=A1+a;
                Fl1=0.001*r*kl;
                hx=(Ft1+Fl1)*cos(alpha*1.0743);
                hy=(Ft1+Fl1)*sin(alpha*1.0743);
                F1x=F1x+hx;
                F1y=F1y+hy;
            else
               break
            end
         alpha=alpha+0.001;
        end
    Lc1=(alpha*r)-(alpha1*r);
end
%Region                                                                  2
if                                                                      Ap>Y
    d=Ap-Y;
    Lc2=d/cos(th2);
    A2=Lc2*f*cos(th2);
    while                                                               s<=Lc2
        a2=f*cos(th2)*0.001;
        Ft2=a2*k;
        at2=at2+a2;
        Fl2=0.001*kl;
        km=-0.0163+0.6299*(s+Lc1)+0.0013*V;
        fx2=(Ft2+Fl2)*cos(th2*km);
        fy2=(Ft2+Fl2)*sin(th2*km);
        F2x=F2x+fx2;
        F2y=F2y+fy2;
        s=s+0.001;
    end
end

%Region3
if                                                                      Ap>Y
    if                                                                  t>0
        ht=f3*cos(th2);
        a3=ht*0.001;
        Ft3=a3*k;
        A3=A3+a3;
        f3x=Ft3*cos(th2*km);
        f3y=Ft3*sin(th2*km);
        F3x=F3x+f3x;
        F3y=F3y+f3y;
    end
    t=t-0.001;
    f3=t/sin(-th2);
end
%Sumation                                  of                            forces
Fx=F1x+F2x+F3x;
Fy=F1y+F2y+F3y;
Lc=Lc1+Lc2;
end
```

10.4. Experimental tests results

10.4.1. TNMG 16 04 04-MF

The experimental results from the insert TNMG 16 04 04-MF are the following,

With a feed rate of 0,1 mm/rev:

A_P	THRUST FORCE (N)	RADIAL FORCE (N)	TANGENTIAL FORCE (N)
0,1	12,25	34,5	41,5
0,2	32,5	51	68,5
0,3	49	67	99
0,4	79,5	77	128,5
0,5	98,5	81	158
0,6	121	80	185
0,7	141	81	216
0,8	162	81	246
1	202	80	292
1,2	240	83	341

Table 3: Experimental cutting forces for insert TNMG 16 04 04-MF and a feed rate of 0,1 mm/rev

With a feed rate of 0,16 mm/rev:

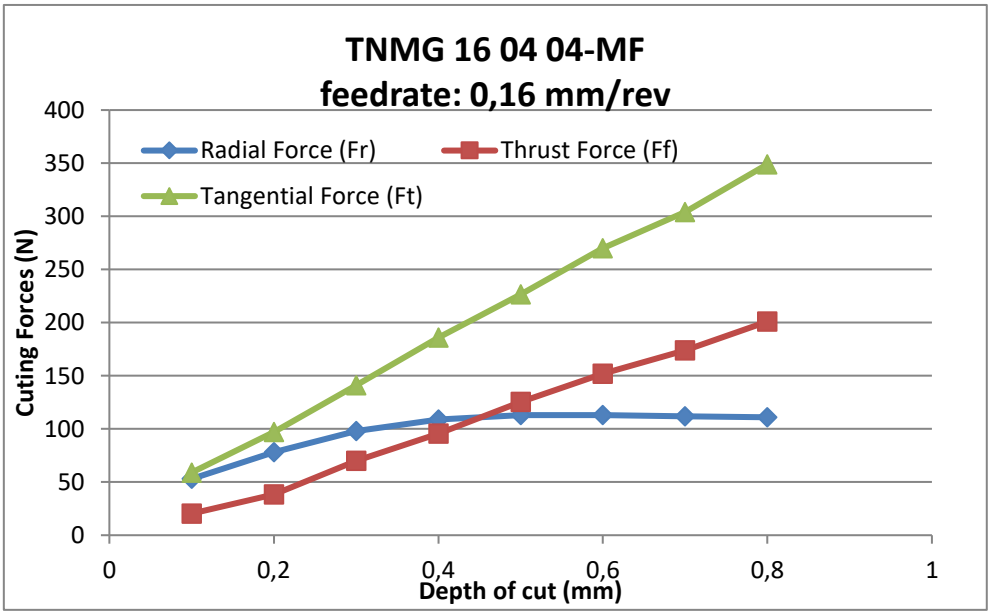

Figure 40: Graphical representation of cutting forces for the insert TNMG 16 04 04-MF and 0,16 mm/rev

A_P	THRUST FORCE (N)	RADIAL FORCE (N)	TANGENTIAL FORCE (N)
0,1	20,333	53	59
0,2	38,5	78	97
0,3	70	98	141
0,4	95,5	109	186
0,5	125,5	113	226,5
0,6	152	113	270
0,7	174	112	304
0,8	201	111	349
1	244	108	423
1,2	311	117	488

Table 4:Experimental cutting forces for the insert TNMG 16 04 04-MF and 0,16 mm/rev

10.4.2. TNMG 16 04 08-MM

The experimental results from the insert TNMG 16 04 08-MM are the following,

With a feed rate of 0,1 mm/rev:

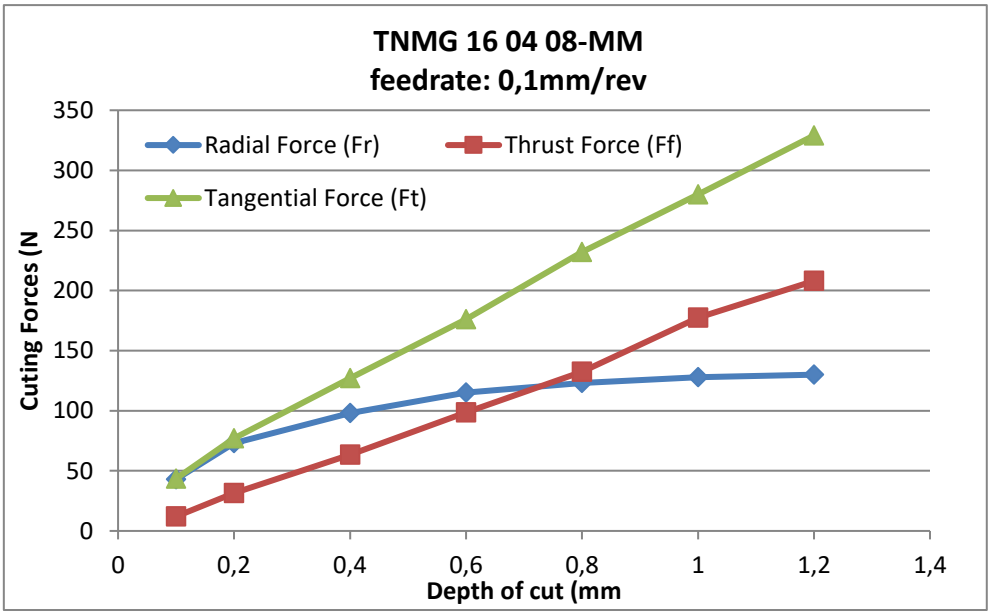

Figure 41: Graphical representation of cutting forces for the insert TNMG 16 04 08-MM and 0,1 mm/rev

A_P	THRUST FORCE (N)	RADIAL FORCE (N)	TANGENTIAL FORCE (N)
0,1	12	43	43,5
0,2	31,5	73	77
0,4	63,33	98	127
0,6	98,5	115	176
0,8	132,5	123	232
1	177,5	128	280
1,2	208	130	329
1,4	237,5	134	363,5

Table 5: Experimental cutting forces for the insert TNMG 16 04 08-MM and 0,1 mm/rev

With a feed rate of 0,2 mm/rev:

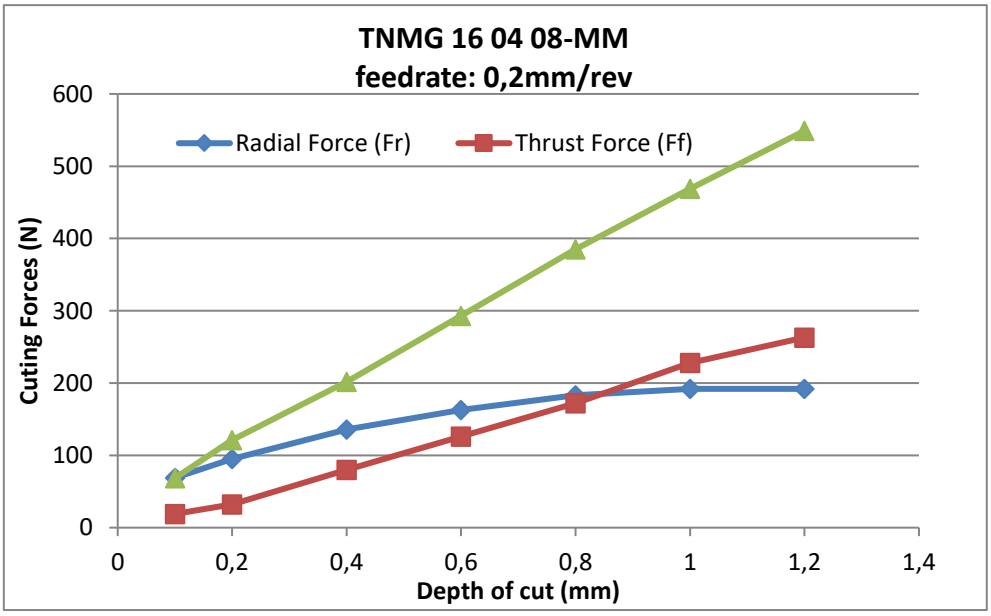

Figure 42: Graphical representation of cutting forces for the insert TNMG 16 04 08-MM and 0,2 mm/rev

A_P	THRUST FORCE (N)	RADIAL FORCE (N)	TANGENTIAL FORCE (N)
0,1	19	69	68,5
0,2	32	95	121
0,4	80	136	202
0,6	126	163	293
0,8	172	183	385
1	228	192	469
1,2	263	192	549
1,4	320	200	636

Table 6: Experimental cutting forces for the insert TNMG 16 04 08-MM and 0,1 mm/rev

10.4.3. RCMT 12 04 M0 235

Experimental results of the RCMT 12 04 M0 235 insert, with a feed rate of 2,4 mm/rev:

A_P	THRUST FORCE (N)	RADIAL FORCE (N)	TANGENTIAL FORCE (N)
0,2	64	444,5	273,5
0,4	77	471	351
0,6	145,5	657	496
0,8	202	756	602
1,2	285	790	799
1,6	379	879	983
2	504	1013	1191
2,4	645	1221	1454

Table 7: Experimental cutting forces for the insert RCMT 12 04 M0 235 and 0,24 mm/rev